Published in final edited form as:
Nature. 2017 July 13; 547(7662): 213–216. doi:10.1038/nature23009.

Nutrient sensing modulates malaria parasite virulence

Liliana Mancio-Silva[1], **Ksenija Slavic**[1], **Margarida T. Grilo Ruivo**[1], **Ana Rita Grosso**[1], **Katarzyna K. Modrzynska**[2], **Iset Medina Vera**[1], **Joana Sales-Dias**[1], **Ana Rita Gomes**[2], **Cameron Ross MacPherson**[3], **Pierre Crozet**[4], **Mattia Adamo**[4], **Elena Baena-Gonzalez**[4], **Rita Tewari**[5], **Manuel Llinás**[6], **Oliver Billker**[2], and **Maria M. Mota**[1,*]

[1]Instituto de Medicina Molecular, Faculdade de Medicina da Universidade de Lisboa, 1649-028 Lisboa, Portugal

[2]Wellcome Trust Sanger Institute, Hinxton, Cambridge CB10 1SA, UK

[3]Institut Pasteur, F-75724 Paris, France

[4]Instituto Gulbenkian de Ciência, Oeiras, Portugal

[5]School of Life Sciences, Queens Medical Centre, University of Nottingham, Nottingham, UK

[6]Department of Biochemistry and Molecular Biology, Department of Chemistry, Center for Malaria Research, and Center for Infectious Disease Dynamics, The Pennsylvania State University, State College, Pennsylvania 16802, USA

Abstract

The lifestyle of intracellular pathogens, such as malaria parasites, is intimately connected to that of their host(s), primarily for nutrient supply. Nutrients act not only as primary sources of energy but also as regulators of gene expression, metabolism and growth, through various signaling networks that confer to cells the ability to sense and adapt to varying environmental conditions1,2. Canonical nutrient-sensing pathways are presumably absent in the causing agent of malaria *Plasmodium*3–5, thus raising the question of whether these parasites possess the capacity to sense and cope with host nutrient fluctuations. Here, we show that *Plasmodium* blood-stage parasites actively respond to host dietary calorie alterations through a rearrangement of their transcriptome accompanied by a significant adjustment of their multiplication rate. A kinome analysis combined with chemical and genetic approaches identified KIN as a critical regulator that mediates sensing

*Correspondence: mmota@medicina.ulisboa.pt.

Author contributions
L.M.S. and M.M.M. conceived and led the study. O.B., M.L., and E.B.G. contributed ideas and interpretation. Animal work was conducted by L.M.S., K.S., M.T.G.R., I.M.V., and J.S.D. Parasite transfections and analysis were performed by L.M.S., K.S., M.T.G.R., and A.R.G.2. Transcriptomic analysis was carried out by A.R.G.1, K.K.M., C.R.M, L.M.S, and M.T.G.R. Yeast complementation studies were performed by K.S., M.T.G.R. and M.A. AMPK modeling was performed by P.C.. R.T. and O.B. provided reagents.

Conflict of interest
The authors declare no conflict of interest.

Data Availability Statement
All expression data (microarray and RNAseq) are available from the Gene Expression Omnibus database under the accession number GSE69629.

Europe PMC Funders Author Manuscripts

of nutrients and controls a transcriptional response to the host nutritional status. KIN shares homology to SNF1/AMPKα and yeast complementation studies suggest functional conservation of an ancient cellular energy sensing pathway. Overall, these findings reveal a key parasite nutrient-sensing mechanism that is critical to modulate parasite replication and virulence.

Europe PMC Funders Author Manuscripts

To establish the impact of host-derived nutrients on the dynamics of malaria infection we applied a long-term moderate caloric restriction (CR) protocol (30-40% reduction in calorie intake, without changes in any dietary component, for 2-3 weeks prior to infection) on different rodent malaria models. CR leads to a consistent reduction in body weight, blood glucose levels, lipids and hormones (e.g. insulin), associated with improved health and longevity6–9 (Fig. 1a, Extended Data Fig. 1a-b). CR-fed mice infected with the rodent malaria parasite *Plasmodium berghei* (mosquito bite or blood passage) showed a significant suppression of peripheral parasitemia and total parasite load relative to the control AL (*ad libitum*) regimen (Fig. 1b, Extended Data Fig. 1d-k). Attenuated parasitemia and virulence was consistently observed regardless of mouse or parasite genetic background (Extended Data Fig. 1d-j), implying a common effect of host diet on *Plasmodium* spp. infections.

As previously reported for short-term dietary restriction10,11, our CR fed mice did not develop experimental cerebral malaria (ECM), resulting in extension of survival (Fig. 1c). ECM protection under short-term CR has been linked to CR-induced changes in inflammation and immunomodulation resulting in reduced parasite accumulation in peripheral tissues and increased parasite clearance in the spleen of mice, with no impact on parasitemia11. However, in the long-term CR condition a general reduction in parasite load was observed with no alterations in parasite body distribution or spleen accumulation (Extended Data Fig. 1k-m). Moreover, severe immunocompromised SCID mice under CR presented attenuated parasitemia (Extended Data Fig. 1j), precluding potential effects of increased clearance.

Having excluded potential redistribution of parasites or increased clearance, we next focused on parasite growth as a possible cause of reduced parasite load in mice under CR regimen. *Plasmodium* parasites replicate inside erythrocytes via schizogony to generate infectious forms called merozoites. Microscopic analysis of parasite development in mice under CR revealed a significant decrease in the mean number of merozoites formed per schizont (Fig. 1d) in *P. berghei* ANKA or *P. berghei* K173 (an isolate that naturally presents high percentage of circulating schizonts12). This observation was recapitulated in an *in vitro* setting, where early stage rodent malaria parasites, as well as the human malaria parasite (*Plasmodium falciparum*) were cultured in medium supplemented with either CR or AL sera (Fig. 1e). Reduction of merozoites formation under CR was further corroborated with other methods such as flow cytometry and luminescence analysis (Fig. 1f, Extended Data Fig. 2a-e). Altogether, these data imply that *Plasmodium* spp. have an intrinsic capacity to respond to a nutrient poor environment by reducing their replicative fitness, thereby lowering total parasite load (Extended Data Fig. 2f-h).

To understand the molecular basis of parasite response to CR, we performed global gene expression profiling from synchronized *P. berghei* parasites under CR or AL regimens, which unveiled a transcriptional reprogramming across the analyzed developmental stages

(Extended Data Fig. 3a-c). Differential expression was validated by qPCR (Extended Data Fig. 3d-e) and functional enrichment analysis revealed a dynamic parasite response to CR (Extended Data Fig. 3f). While functions related to regulation of gene expression and signaling (including a number of kinases) were induced, functions related to parasite maturation and replication, such as ion transport, DNA replication, and cell cycle were repressed. The repression of functions critical to intraerythrocytic development is consistent with the reduced growth CR phenotype and is in agreement with a response to nutrient limiting environments observed for other organisms13.

Given the overrepresentation of protein kinases in the transcriptomic analysis (Extended Data Fig. 3f) and their prominent role in eukaryotic nutrient sensing2 we set out to identify parasite kinases implicated in the CR response. We utilized the *in vitro* maturation assay to screen *P. berghei* kinase mutant lines14 and identified NEK4, PK7 and KIN as unresponsive to CR (Fig. 2a, Extended Data Fig. 4a). While Δ*nek4* and Δ*pk7*15 produced a reduced number of merozoites regardless of AL or CR conditions, Δ*kin* parasites in CR generated merozoite numbers comparable to wild-type parasites in AL (Fig. 2a-b, Extended Data Fig. 4b). We further examined Δ*kin* parasites *in vivo* under both dietary regimens and observed no significant differences in parasitemia during the first days of infection, when parasite growth is linear (Fig. 2c). From day 4 onwards, Δ*kin* parasites outgrew wild-type in both dietary conditions, but presented lower parasitemia in CR compared to AL mice (Extended Data Fig. 4e), suggesting that additional parasite molecules may control growth at this point of infection. It is also possible that nutrient levels in AL mice become suboptimal at high parasitemia, which might prevent growth of wild-type but not Δ*kin* parasites, implying that KIN may also be responsive to parasite density16. Of note, the Δ*kin* phenotypes, *in vitro* and *in vivo,* were rescued by complementation with the *kin* gene (Δ*kin+kin*, Fig. 2b-c, Extended Data Fig. 4c-e). Remarkably, a lack of CR-transcriptional response was observed in Δ*kin* parasites (Fig. 2d, Extended Data Fig. 4f-i), further substantiating the role of KIN in orchestrating a response to environmental nutritional changes.

KIN is a putative serine/threonine kinase, with limited homology to the conserved family of sucrose non-fermenting 1 (SNF1) and AMP-activated kinases (AMPK)4,14,17 that regulate cellular energy homeostasis in yeast and mammalian cells, respectively18,19. AMPK/SNF1 is a heterotrimeric complex comprising a α-catalytic subunit and two regulatory subunits β and γ. While avian *Plasmodium* spp. genomes encode homologues to α, β and γ subunits20, mammalian *Plasmodium* spp. seem to have lost the heterotrimeric complex and only retained KIN as a plausible AMPKα-related protein kinase4,14. It is still possible that cryptic β and γ subunits exist but remain to be identified or that the poorly conserved N and C-terminal extensions serve these functions (Extended Data Fig. 5a). Homology of *P. berghei* and *P. falciparum* KIN to the AMPKα subunit is confined to the kinase domain, which includes a conserved threonine residue in the activation loop (T616 in PbKIN, Extended Data Fig. 5a-b), whose phosphorylation is essential for SNF1/AMPK activity19, and replacement of this threonine by an aspartic acid residue has been validated as a phosphomimetic21. To investigate the possible impact of KIN activation on parasite replication, we engineered a parasite in which the T616 was replaced by aspartic acid. Parasites expressing PbKIN^{T616D} generated fewer merozoites and lower parasitemia in mice under AL conditions, appearing to closely phenocopy the CR response of wild-type parasites

(Fig. 2e-f, Extended Data Fig. 5c-e). Moreover, the T616D phosphomimetic mutation was essential to complement the yeast Δ*snf1* mutant. Expression of the PbKIN^{T616D} variant in Δ*snf1*, but not the wild-type PbKIN^{T616} or N-terminal truncated versions, rescued yeast growth nearly to the extent of wild-type SNF1 (Fig. 2g-h, Extended Data Fig. 5f-g). While these results imply that targets downstream of KIN are at least partly conserved, the failure to rescue Δ*snf1* with KIN^{T616} indicates that upstream regulatory kinases have likely diverged or that the active complex is not correctly assembled in yeast. These results point towards a functional conservation of KIN with the AMPK/SNF1 family of kinases.

We next tested whether parasites would respond to direct AMPK activating compounds. Despite the lack of a clear homologue for the AMPKβ subunit (known to interact with salicylate and A769662 to promote and maintain phosphorylation in the AMPKα activation loop22–24), both *P. berghei* and *P. falciparum* parasites responded to treatments in a dose-dependent manner *in vitro*, with reduction in merozoite formation in wild-type but not in Δ*kin* parasites. Other kinase-deficient parasite lines as well as the Δ*kin+kin* responded to treatment as wild-type parasites (Fig. 2i, Extended Data Fig. 6a-e). *In vivo* daily administration of salicylate led to decreased parasitemia in mice infected with wild-type and Δ*kin+kin* parasite lines but not in Δ*kin*-infected mice (Extended Data Fig. 6f-g).

AMPK/SNF1 kinases are activated under conditions of energy deficiency. Sugars that are metabolized, such as glucose, suppress their activation18,19. The effect of CR sera on parasite replication was abolished by glucose addition in a KIN-dependent manner (Fig. 3a-b). Glucose also reverted the salicylate effect in *P. berghei* and *P. falciparum* (Fig. 3a, Extended Data Fig. 7a-b). Supplementation with other nutrients (vitamins, non- and essential amino acids, iron) or leptin (altered under CR11,25), did not affect parasite sensitivity to salicylate or A769662 (Extended Data Fig. 7b-d). Furthermore, *in vivo* glucose supplementation, which increased blood glucose levels and mouse weight in CR fed mice, lead to increased parasitemia and antagonized the CR-induced parasite gene repression (Fig. 3c-d, Extended Data Fig. 7e-g). These data demonstrate that glucose can suppress a nutrient-sensing signaling cascade requiring KIN activation.

P. falciparum malaria cases arising in patients shortly after their arrival at a hospital have been associated with increased parasitemia upon re-feeding after famine26. We recapitulated these observations in an experimental setting by changing the mice diet from CR to AL during an ongoing infection and observed immediate body weight gain, concomitant with increased parasitemia (Fig. 3e-f). Alternatively, parasites transferred from CR mice into naïve AL mice led to increased parasitemia and premature death due to ECM (Fig. 3g). These results together with previous observations in humans26 provide strong evidence that malaria parasites rapidly adjust their replicative capacity based on nutrient availability. The data presented here reveal that despite the lack of the canonical nutrient-sensing pathways, *Plasmodium* parasites encode an unusual AMPK/SNF1 homologue (KIN) that acts as a nutrient sensor, driving a fast and coordinated response, prior to any nutrient becoming limiting. The question that arises is what triggers the parasite's immediate response to diminishing nutrient availability? Intracellular and extracellular nutrient and micronutrient levels such as sugars, amino acids, lipids and surrogate metabolites, iron and zinc, or global energy levels are known to serve as signals for cells to sense their environment1. While the

rescue by glucose supplementation could suggest that glucose is the primary signal for parasite growth, the range of variation of glucose levels in rodent blood is small (6 and 4 mM for AL and CR, respectively) and only high levels of glucose (50 mM) revert the CR effect *in vitro*. By contrast, parasites in AL can develop in low glucose (<2.5mM), indicating that AL serum contains the components that are necessary and sufficient to suppress KIN activity and allow high parasite replication. Altogether, the data favors a model where energy alterations derived from changes in the nutrient status of the host are sensed by the parasite via KIN (Extended Data Fig. 8).

This study reveals a missing link between the host nutrient status and parasite growth, which might be highly relevant given the alarming trend of global increase in overweight populations, including malaria endemic regions27. It puts forward the possibility of targeting parasite nutrient-sensing mechanisms as an approach to attenuate parasite replication and virulence. It also uncovers a potential strategy utilized by the parasite to modulate its transmission. Dry seasons create parasite transmission bottlenecks, with the endemic populations carrying, asymptomatically, low parasite burden28. It is tempting to propose that parasite nutrient-sensing may be critical to ensure parasite survival and persistence in hosts living in areas where *Plasmodium* is seasonally transmitted.

Methods

Chemicals and Reagents

Salicylate (71945), glucose free RPMI 1640 (R1383), MEM essential amino acids (M5550), and MEM vitamin solution (M6895), Glucose (G6152) were obtained from Sigma. RPMI 1640 (31870), HEPES (15630), Penicillin Streptomycin (15140), Gentamicin (15750), MEM non-essential amino acids (11140), Fetal Bovine Sera (10500), Albumax II (11021-029), and SYBR green I (S7585) were purchased from Life Technologies. A769662 (171258) was purchased from Calbiochem. Mouse recombinant leptin was obtained from R&D Systems (498-OB). Anti-GFP from mouse $IgG_1\kappa$ (clones 7.1 and 13.1) was purchased from Roche (11814460001).

Animals and Diets

Animal research was conducted at the Instituto de Medicina Molecular (Lisboa, Portugal). All experiments were approved by the animal ethics committee at the institute and performed according to national and European regulations. Rodents were purchased from Charles River (Spain). SCID mice were kindly provided by João Barata (Instituto de Medicina Molecular).

Experimental mice (age 5-8 weeks; males; weight 18-28 g) were housed three to five per cage. Rats (males, weight 200-500g) were housed one to two per cage. Animals were assigned to the different experimental groups based on body weight (assuming that mice of similar weight have comparable food intake). After grouping animals by weight, they were randomly assigned to AL or CR. Animals were allowed free access to water and food except for the groups on calorie restriction (CR). Mice and rats on CR were given daily 60-70% of the food consumed by the control group *ad libitum* (AL). Food intake in both groups was

measured daily and body weights at least 3 times a week. Blood glucose levels were monitored regularly in mice and rats with the ACCU-CHEK glucose meter (Roche), using one droplet of tail blood. Upon reaching 15-20% weight loss, the daily food allotted to CR mice or rats was adjusted to stabilize the lower body weights for the remainder of the experimental period. Blinding was not possible as mice under CR exhibit a clear difference in size. For drug treatments, mice were first grouped by body weight and then randomly assigned to receive treatment or vehicle control.

Parasite Lines

P. berghei ANKA (GFP_{con}, 259cl2; $GFP\text{-}Luc_{con}$, 676m1cl1; $GFP\text{-}Luc_{schiz}$, 1037cl1) and *P. berghei* K173 (1006cl1) parasite lines were obtained from the Leiden Malaria Research Group (www.pberghei.eu). *P. chabaudi chabaudi* AS was kindly provided by Jean Langhorne (National Institute for Medical Research, London, UK). *P. yoelii* 17X NL and *P. falciparum* 3D7 were obtained through the MR4 (www.mr4.org). *P. berghei* kinase deficient lines were generated previously13. *P. berghei* KIN^{T616}, KIN^{T616D} and Δ*kin* complementation were obtained by double crossover recombination as described in Extended Data Fig. 5c and 4c, respectively. Transfections were done by electroporation of purified schizonts29. Parasites were harvested on day 7-10 post transfections and genotyped by PCR, with the primers listed in Supplementary Table 1. Knockout and complemented parasite lines were dilution cloned before further experimentation.

Animal Infections

Mouse infections were achieved by exposing mice to infected *Anopheles stephensi* mosquitoes (5 mosquitoes/mouse, for 30 minutes), or by intraperitoneal (i.p.) inoculation of 1×10^6 or 1×10^5 infected RBCs (iRBC) into C57BL/6 or BALB/c mice, respectively. iRBC were obtained by prior passage in the correspondent C57BL/6 or BALB/c mice. For synchronized infections, BALB/c mice were infected by intravenous (i.v.) injection of $5\text{-}10x10^8$ purified mature schizonts, obtained after parasite *in vitro* maturation30.

For GFP-expressing parasites, parasitemia was determined daily by flow cytometry analysis of one drop of tail blood as described below. For non-GFP expressing parasite lines, the course of parasitemia was monitored on Giemsa stained blood smears. Images of 1-10 thousand RBCs were randomly acquired and the percentage of iRBC counted semi-automatically using ImageJ (http://rsbweb.nih.gov/ij). Luciferase expressing parasites were visualized live in the whole body of animals using an intensified-charge-coupled device photon-counting video camera from the IVIS Lumina (Caliper LifeSciences) after subcutaneous injection of D-luciferin (100mg/Kg).

Serum Preparation

AL and CR sera were prepared from Wistar rats or BALB/c mice on AL or CR for at least 30 days. Whole blood was collected from animals by cardiac puncture and left at room temperature for 30 minutes to clot. After a 10-minute centrifugation at 2000g 4°C, the resulting supernatant was aliquoted and stored at -80°C. Sera were heat inactivated for 30 minutes at 56°C, chilled on ice and added to the culture media immediately prior use. Blood

glucose levels in rats prior sample collection were as follows: AL, 105±11.3 mg/dL (6mM) and CR, 69±7.1 mg/dL (4mM).

in vitro Maturation Assays

Blood stages of rodent malaria parasites can only be maintained *in vitro* for one developmental cycle. CR *in vitro* assay consisted in allowing parasites to mature from rings/young trophozoites into segmented schizonts in culture medium supplemented with AL or CR sera, instead of standard Fetal Bovine Sera (FBS), as outlined in Extended Data Fig. 2a. AL and CR sera were obtained from mice or rats, but most of the experiments were performed using the rat serum, because it could be obtained in higher amounts. *P. berghei* and *P. yoelii* parasites were collected from the tail of infected mice at 0.5-2% parasitemia, washed in warmed incomplete glucose free RPMI, and added to 96-well plates with complete culture medium (glucose free RPMI supplemented with 4-5mM glucose, 25mM HEPES, 2g/L $NaHCO_3$, 50μg/L Gentamicin and 10-25% AL or CR sera) at 1% hematocrit (final volume 100μl). Plates were incubated at 37°C in an atmosphere of 5% O_2, 5% CO_2 and 90% N_2 for 22-30 hr. Most of the experiments, including the kinome screen (Fig. 2a), were performed with 25% sera and 4mM glucose, which makes the final concentration of glucose in the medium of approx. 4.5mM for AL and 4.0mM for CR. The luminescence assays (and Fig. 3b) were performed with 10% sera and 5mM glucose in the base medium, making the final glucose concentration 5.1mM for AL and 4.9mM for CR.

Mature schizonts were visualized by microscopy after Dapi or Giemsa staining and quantified manually or automatically using ImageJ counter tools (30-50 segmented schizonts with a single hemozoin pigment and clearly separated merozoites were scored per condition). Some experiments were scored by different investigators blindly. Alternatively, the GFP-expressing parasites were analyzed by flow cytometry (as described in Extended Data Fig. 2e), or luciferase-expressing parasites (in schizont stage only) were assessed by luminescence assays (as described below).

For *P. falciparum* parasites, we replaced the lipid-rich bovine serum albumin (Albumax II) by AL or CR rat sera. Mixed stage parasites were allowed to mature into schizonts in RPMI based medium containing 5mM glucose, 25mM HEPES, 2g/L $NaHCO_3$, 100μM Hypoxanthine, 50μg/L Gentamicin and 10% AL or CR rat sera, in 96-well plates. Initial parasitemia was set to 1% and hematocrit to 2%. Plates were incubated at 37°C as described above. Parasite samples were collected, fixed and Giemsa stained at multiple time-points (24-30 hr later). Blood smears were examined by microscopy as detailed above for rodent parasites.

Drug Treatments *in vitro*

Drugs and vehicles (as control) were dispensed into a 96-well plate in duplicates with a series of 2-fold dilutions. The parasite suspension was then added to the plates and incubated at 37°C in 5% O_2, 5% CO_2 and 90% N_2 for 24 hr (*P. berghei*) or 48 hr and 96 hr (*P. falciparum*). *P. berghei* parasites were cultured in glucose free RPMI supplemented with 5mM glucose, 25mM HEPES, 2g/L $NaHCO_3$, 50μg/L Penicillin Streptomycin and 25% FBS at 1% final hematocrit. The drug effect on schizont development was examined at 24 hr by

Europe PMC Funders Author Manuscripts

microscopy, or luminescence as detailed below. Ring stages of *P. falciparum* were cultured in standard RPMI (11mM glucose), 25mM HEPES, 100μM Hypoxanthine, 2mM L-glutamine, 50μg/L Gentamicin and 0.5% Albumax II at 2% hematocrit and starting parasitemia adjusted to 0.1%. Parasitemia after 48 hr and 96 hr was analyzed by flow cytometry after SYBR Green staining and EC50 values calculated by fitting the data to a log dose-response curve using GraphPad (Prism).

Luminescence Assay

Supernatants were carefully removed from the 96-well plates at 24 hr after incubation and the cells were re-suspended in 50μl of lysis buffer (Firefly Luciferase Assay Kit, Biotium). Plates were then shaken for 15 minutes. Luminescence was determined by adding 50 μL of D-luciferin (200ng/mL) in Firefly Luminescence Buffer to 30 μL of total lysate in white 96-well plates and immediately measured using a multiplate reader (Infinite 200M, Tecan). Values of luciferase activity are expressed as relative luminescence units.

Flow Cytometry

Flow cytometry analysis was used to determine the parasitemia in mice (for *P. berghei* GFP-expressing parasites), parasitemia in *P. falciparum in vitro* cultures (after staining with SYBR Green), and schizont development (for *P. berghei* GFP-expressing parasite lines after *in vitro* maturation). *P. berghei* GFP-expressing parasites were analyzed on BD FACSCAlibur or BD LSRFortessa equipment. The number of total acquired events ranged from 1-2 million (days 1-3 of infection) to 100-200 thousand (onwards). To assess schizont development 100-200 thousand events/condition were acquired. *P. falciparum* SYBR Green stained samples were analyzed on CyFlow SL Blue or BD Accuri C6 instrument (100-200 thousand events/condition). The data was further analyzed on FlowJo (TreeStar). RBCs were selected on the basis of their size by gating first on FSC and SSC and, subsequently, on FITC/FL1 and PE/FL3 channels (to eliminate false positives associated to RBC auto-fluorescence). iRBC were detected in the FITC/FL1 channel.

Yeast Complementation Assays

A codon-optimised version of *P. berghei* KIN ORF (GenScript, USA Inc.) was used for expression in *Saccharomyces cerevisiae* Δ*snf1* mutant31. The expression plasmid was constructed by cloning the KIN ORF without the stop codon as BamHI-NotI fragment into the expression vector pRS426, containing the Ura selectable marker. Subsequently, the GFP coding sequence was cloned in frame with KIN ORF as a NotI-SacI fragment. The T616D mutation was introduced into the codon-optimized KIN ORF by site-directed mutagenesis. All the generated plasmids were transformed into Δ*snf1* using a previously described Li–acetate method and selected on SD medium lacking uracil32. The sequences of primers used for cloning are given in Supplementary Table 1.

Western Blot Analysis

Whole cell extracts were prepared by the following procedure: overnight cultures of Δ*snf1*-transfected strains were harvested by centrifugation and washed by shaking at 30°C for 15 minutes in buffer containing 0.1 M Tris pH 9.4, 50 mM 2-mercaptoethanol and 0.1 M

glucose; cells were then treated with lyticase to digest the cell wall in buffer containing 0.9 M sorbitol, 0.1 M glucose, 50 mM Tris pH 8, 5 mM dithiothreitol and 0.5x SD media for 1 hr at 30°C. After washing in 1M sorbitol, cells were lysed in NuPAGE LDS loading buffer and 5 μg of protein were separated by SDS-PAGE in a Any kD mini-protean precast gel (Biorad). Protein transfer to a nitrocellulose membrane was performed overnight at 4°C in buffer containing 6.03 g/l Tris and 3.09 g/l Boric acid, at 30V with constant voltage. Blocking was done in TBS-5% milk Tween 0.2% for 1 hr at room temperature. The membrane was then incubated with primary anti-GFP antibody diluted 1:1000 in TBS-5% milk Tween 0.2% for 3 hr at room temperature. Secondary antibody was goat anti-mouse HRP conjugated antibody (Jackson ImmunoResearch), diluted 1:5000 in TBS-5% milk Tween 0.2% and incubated for 1 hr at room temperature.

Microarray Analysis

Transcriptional profiling of synchronized parasites across the developmental cycle in AL and CR was performed using DNA microarrays. To prepare the samples, we started by transferring the blood of a BALB/c infected mouse (>10% parasitemia) into 3 Wistar rats by intraperitoneal injection. When the parasitemia was 1-3%, the blood was collected by cardiac puncture (with heparin) and cultured overnight (standard RPMI supplemented with 25 mM HEPES, 50 μg/L Gentamicin and 25% FBS). The mature schizonts obtained *in vitro* were separated from uninfected cells by Nycodenz-density gradient centrifugation and injected intravenously (tail) into BALB/c mice that were under AL or CR, as outlined in Extended Data Fig. 3a. The parasites were allowed to go through one developmental cycle in the new hosts and samples started to be collected with 4 hr intervals on the second cycle. Giemsa staining on thin blood smears was performed for each collecting point and parasite area (as proxy for parasite age33) was scored using ImageJ. The blood from 3 mice per condition was collected by cardiac puncture, washed in warm RPMI, filtered through Plasmodipur (EuroProxima) to remove mouse leukocytes, lysed in PureZOL (Bio-Rad) and stored at -80°C. RNA was then extracted with chloroform, precipitated overnight at -20°C with isopropanol, washed with ethanol, and stored at -80°C.

Total RNA was primed with a mix of OligodT and random primers for 10 minutes at 70°C, and reverse transcribed with Superscript III (Life Technologies) with amino-allyl dUTP (Ambion) for 2 hr at 50°C. After purification, samples and references (pool of cDNA samples) were labeled with cy5 and cy3 (Amersham), respectively, and hybridized on the *P. berghei* Agilent nuclear expression array. The microarray contain approximately 14000 probes targeting 5850 transcripts, with an average of 2.5+ probes per transcript34.

The raw data was pre-processed and normalized with ‘limma’ package (http://www.bioconductor.org/packages/release/bioc/html/limma.html), using the following methods: minimum for background correction, loess for normalization within microarrays and aquantile for normalization between microarrays. Linear models were used to obtain the CR and AL control diet expression profiles from the biological replicates at each time-point, as implemented in ‘limma’ package. Differentially expressed genes between CR and AL control diet samples were selected using an absolute fold-change higher than two and FDR adjusted P value cutoff of 0.01. Significant expression alterations were graphically

represented using an MA-plot, showing the log-fold-changes on CR versus AL diet versus the average log-expression values of the two samples at each time point (Extended Data Fig. 3c).

RNA Sequencing

Transcription profiling of synchronized *P. berghei* wild-type and Δ*kin* parasites was performed by RNA sequencing. The samples were obtained as described above (mouse > rat > *ex vivo* culture > mice in AL or CR), but collected at single time-point (10 hr after invasion). The total mRNA was extracted using the PureZOL reagent (Bio-Rad) and Magnetic mRNA Isolation Kit (NEB). First strand cDNA was synthesized with Random Hexamer primers and SuperScript III Reverse Transcriptase (Life Technologies). The DNA/RNA hybrids were purified using Agencourt AMPure XP beads and the 2nd strand was synthesized using dUTP nucleotide mix, DNA Polymerase I (E. coli) and RNAse H by 2.5 hr of incubation at 16°C. cDNA was fragmented to approximately 200 nucleotides using Covaris S220 System. The fragments were end-repaired, TA-tailed and ligated to Illumina adaptors with index barcodes using NEBNext kits according to manufacturer instructions. Excess adaptors were removed with 2 rounds of clean up with 50μl of Agencourt AMPure XP beads (Beckman Coulter). Final libraries were eluted in water, quantified on an Agilent Bioanalyzer 2100 High Sensitivity DNA chip and quantified by qPCR. A pool of the indexed libraries was sequenced on an Illumina HiSeq2500, with 100bp paired-end reads. RNA-seq reads were mapped to the PlasmoDB reference *P. berghei* ANKA genome (www.plasmodb.org) with TopHat2 software using default parameters35. Gene expression levels were obtained using PlasmoDB genome annotations and genes with strong gametocyte signatures (Modrzynska, K.K. and Bilker, O. unpublished) were removed from the analysis. Differential expression was assessed using edgeR and limma R packages36,37. First, the normalization factors were calculated to scale the raw library sizes using edgeR. Second, linear modelling and empirical Bayes moderation were applied to detect differentially expressed genes (thresholds of absolute fold-change higher than two and FDR adjusted P values lower than 0.01). Normalized expression values (RPKMs) were obtained using edge R package38.

qPCR Analysis

Samples prepared above were tested by RT qPCR analysis for data comparison. Additionally, RNA from independent biological samples of asynchronous and synchronized *P. berghei* parasites was extracted as detailed above and DNAse treated (Sigma) prior cDNA synthesis. Alternatively, RNA extracted with PureZOL (BioRad) was coupled with purification on columns including DNAse treatment (NZY Total RNA Isolation kit, NZYTech). Total RNA from *P. falciparum* synchronized cultures was extracted with Trizol and column purification (NZY Total RNA Isolation kit, NZY Tech). DNAse treated RNA was primed with random hexamers and reverse transcribed using NZY First-Strand cDNA Synthesis Kit (NZYTech). Real-time PCR was performed on ABI 7500 or 7900HT systems (Applied Biosystems), using Universal SYBR Green Supermix (Bio-Rad) and the primers listed in Supplementary Table 1. Relative gene expression was normalized to the geometric mean of reference genes PBANKA_061540 and PBANKA_011140 for *P. berghei,* using the ΔΔCt method. *P. falciparum* data was normalized to PF3D7_0717700 gene. Total RNA from

Europe PMC Funders Author Manuscripts

infected spleens was extracted with NZY Total RNA Isolation kit (NZYTech), primed with random hexamers, reverse transcribed and analyzed by qPCR as above. Total parasite load was determined by detecting expression of *P. berghei* 18S rRNA, normalized to mouse *hprt* housekeeping gene using the ΔΔCt method. Primers listed in Supplementary Table 1.

Statistics

Significance was calculated using different tests on the GraphPad (Prism) software. Mann-Whitney U tests for comparisons between two conditions, and two-way ANOVA was used to compare parasitemia between CR or drug treatments and the control group mice. The log-rank (Matel-Cox) test was used to compare the survival distributions of two groups. Significance was considered for p values below 0.05. The outliers in the boxplots represent 10% of data points. Biological replicates (n) indicated in figure legends refers to the number of mice, number of schizonts, or number of independent cultures that were pooled from 1 to 3 experiments performed independently. Sample sizes were chosen on the basis of historical data.

Extended Data

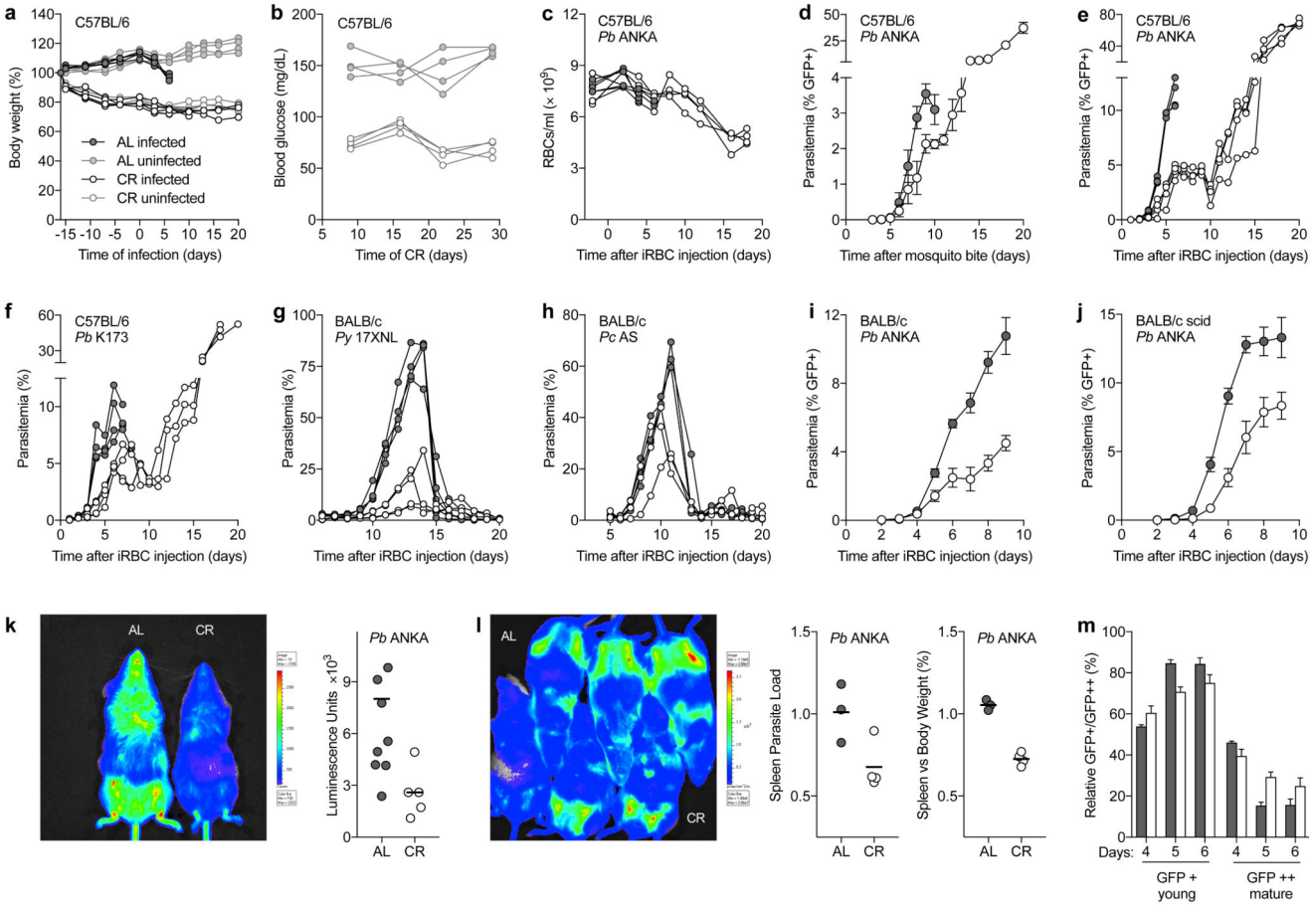

Extended Data Figure 1. Impact of calorie restricted diet in rodent malaria models.

a-b. Body weight change (**a**) and blood glucose levels (**b**) of C57BL/6 male mice under long-term calorie restriction (CR) or *ad libitum* (AL). Body weight data (mean±sd; n=4/group) was normalized to the initial weight for each animal. The average daily food consumption for AL and CR mice was 2.93±0.48g and 1.76±0.11g, respectively (mean±sd).
c. Number of RBCs/ml in infected C57BL/6 male mice in AL and CR diet regimens. Cell density was determined in 1μl of blood collected from the tail and counted on a hemocytometer chamber (mean±sd; n=4/group).
d-f. Full course of parasitemia from infected mice infected by mosquito bite (**d**) or by intraperitoneal (i.p.) injection of 1×10^6 infected RBCs (iRBC) (**e-f**). Values (mean±sem) represent one of 2 independent experiments. Parasitemia of GFP-expressing *P. berghei* ANKA (mosquito bite, n=5/group; iRBC, n=4/group) determined by flow cytometry analysis. Parasitemia of *P. berghei* K173 (n=4/group) obtained by microscopy analysis of blood smears.
g-h. Parasitemia of a representative experiment of male BALB/c mice infected i.p. with 1×10^5 *P. yoelii* 17XNL iRBC (n=4/group) or 1×10^5 *P. chabaudi* AS iRBC (n=3/group). Parasitemia obtained by microscopy analysis represents 1 of 2 independent experiments.
i-j. Parasitemia of *P. berghei* ANKA infection in BALB/c (**i**) and BALB/c scid (severe combined immune deficiency) mice (**j**). Mice were infected by i.p. injection of 1×10^5 GFP-expressing parasites and parasitemia assessed by flow cytometry (mean±sem; BALB/c, n=8/group; BALB/c scid, AL n=7, CR n=8; 2 independent experiments pooled).
k. BALB/c mice i.p. injected with 1×10^5 *P. berghei* ANKA expressing luciferase under a constitutive promotor[30] and imaged on day 4 after infection (AL n=10, CR n=5; 2 independent experiments pooled).
l. BALB/c mice infected with *P. berghei* ANKA expressing luciferase under the *ama1* schizont-specific promoter30, to allow imaging of the sequestering parasite stage. Mice were imaged 25h after i.v. infection with purified mature schizonts. AL, top animals; CR, bottom animals. Spleen weight and parasite load measured 72h after infection with mature schizonts. Parasite load was determined by qPCR analysis of *P. berghei* 18S rRNA. Spleen weight was normalized to body weight for each mouse (AL n=3, CR n=4).
m. Relative abundance of circulating young and mature parasites in AL and CR C57BL/6 mice infected with $1x10^6$ GFP-expressing *P. berghei* ANKA iRBCs. Tail blood from infected mice was analyzed by flow cytometry. After excluding false GFP-positive events, the total GFP population was separated in low (GFP+) and high (GFP++) GFP-expressing cells, corresponding to young and mature parasites, respectively. The same gates were applied to AL and CR blood samples on days 4, 5, and 6 after infection. The observed marked reduction in the percentage of mature parasites overtime in both diet conditions is indicative of sequestration of infected RBCs. Bars are mean±sem (7 mice/group; 2 independent experiments pooled).

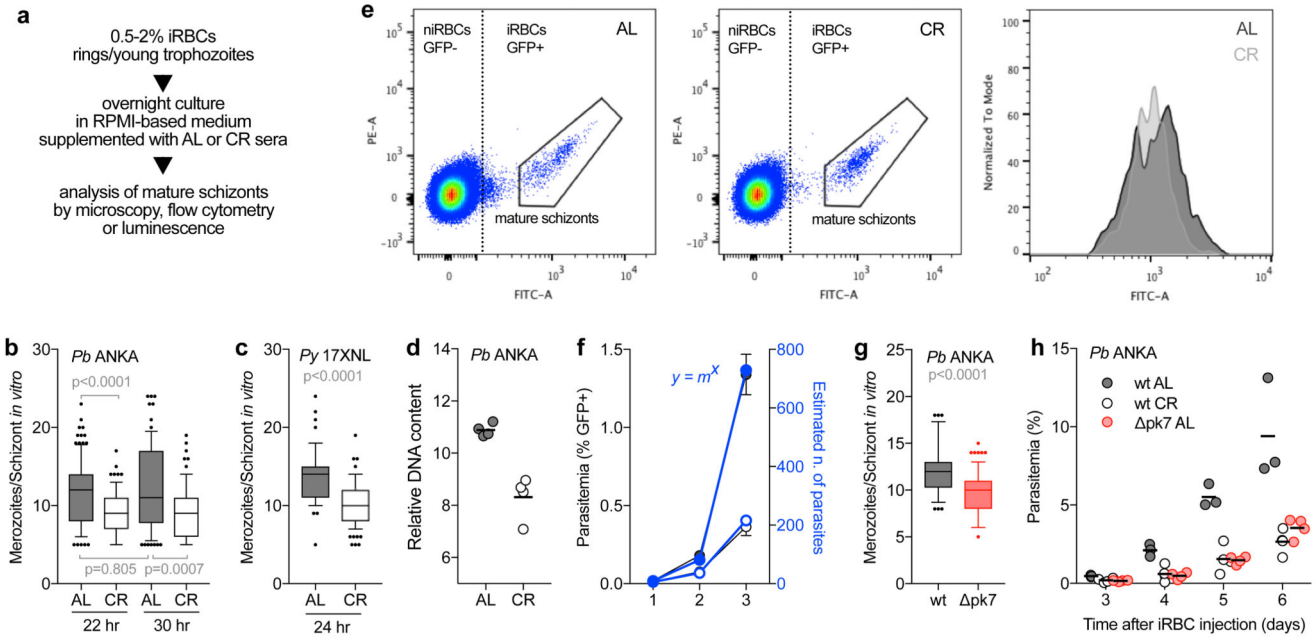

Extended Data Figure 2. Effect of CR *in vitro*.

a. Workflow representation of the *in vitro* parasite maturation assay. Experiments were conducted in a glucose-free RPMI medium supplemented with HEPES, antibiotic, 10-25% rodent sera and glucose at the concentration indicated in the corresponding figure and/or legend.

b-c. Boxplots showing microscopic quantification of the number of *P. berghei* ANKA (**b**) or *P. yoelii* 17XNL (**c**) merozoites per segmented schizont after *in vitro* culturing in the presence of 25% AL or CR mouse sera (glucose, 4mM). Culture for 30 hr showed similarly reduced merozoite numbers in the CR condition, suggesting that parasite development is not delayed in CR. Only mature schizonts with clear separated merozoites and a single pigmented digestive vacuole were imaged and scored (Mann-Whitney test). Total numbers of schizonts analyzed in 2 independent experiments are as follows: *P. berghei* AL 22h, 111; CR 22h, 78; AL 30h, 74; CR 30h, 94; *P. yoelii* AL, 58; CR, 107.

d. Flow cytometry analysis of *P. berghei* ANKA schizonts prepared as in (**b**) and stained with SYBR Green to quantify the DNA content (2 independent experiments).

e. Representative flow cytometry plots and gating strategy for analysis of GFP-expressing *P. berghei* ANKA parasites after 24 hr *in vitro* culture with 25% AL or CR rat sera (glucose, 4mM). Cells were selected on FSC and SSC and then on FITC (green) and PE (red) channels. As shown in left and middle panels, mature schizonts express strong GFP signal detected in the FITC channel. Histogram plot show fluorescent intensity comparison between AL and CR. Data represents 1 of 3 independent experiments.

f. Comparing parasitemia levels (left axis, black) and the estimated parasite numbers (right axis, blue) using a geometric progression ($y=m^x$) in which the basis is the mean merozoite number for AL and CR (9 and 6, respectively) for the first days of parasite linear growth. Parasitemia data was obtained from Fig. 2c (mean±sem; n=11/group; AL, closed circles, CR open circles). Matematical modeling of parasitemia taking into account only the number of

Europe PMC Funders Author Manuscripts

merozoites appears to be sufficient to predict the observed growth difference of *P. berghei* during early infection.

g-h. Boxplot of merozoite numbers and parasitemia of *P. berghei* ANKA wild-type (wt) and Δ*pk7* parasites. Number of schizonts analyzed after *in vitro* maturation in AL conditions in 2 independent experiments are as follows: wt, 36; Δ*pk7*, 85. **h**. Parasitemia determined by microscopic examination of blood smears from C57BL/6 mice infected with $1x10^6$ iRBCs of *P. berghei* ANKA Δ*pk7* (n=4) and the parental wt (AL n=3; CR n=4). The data show that parasites producing fewer merozoites lead to similar low parasitemia to that of parasites under CR.

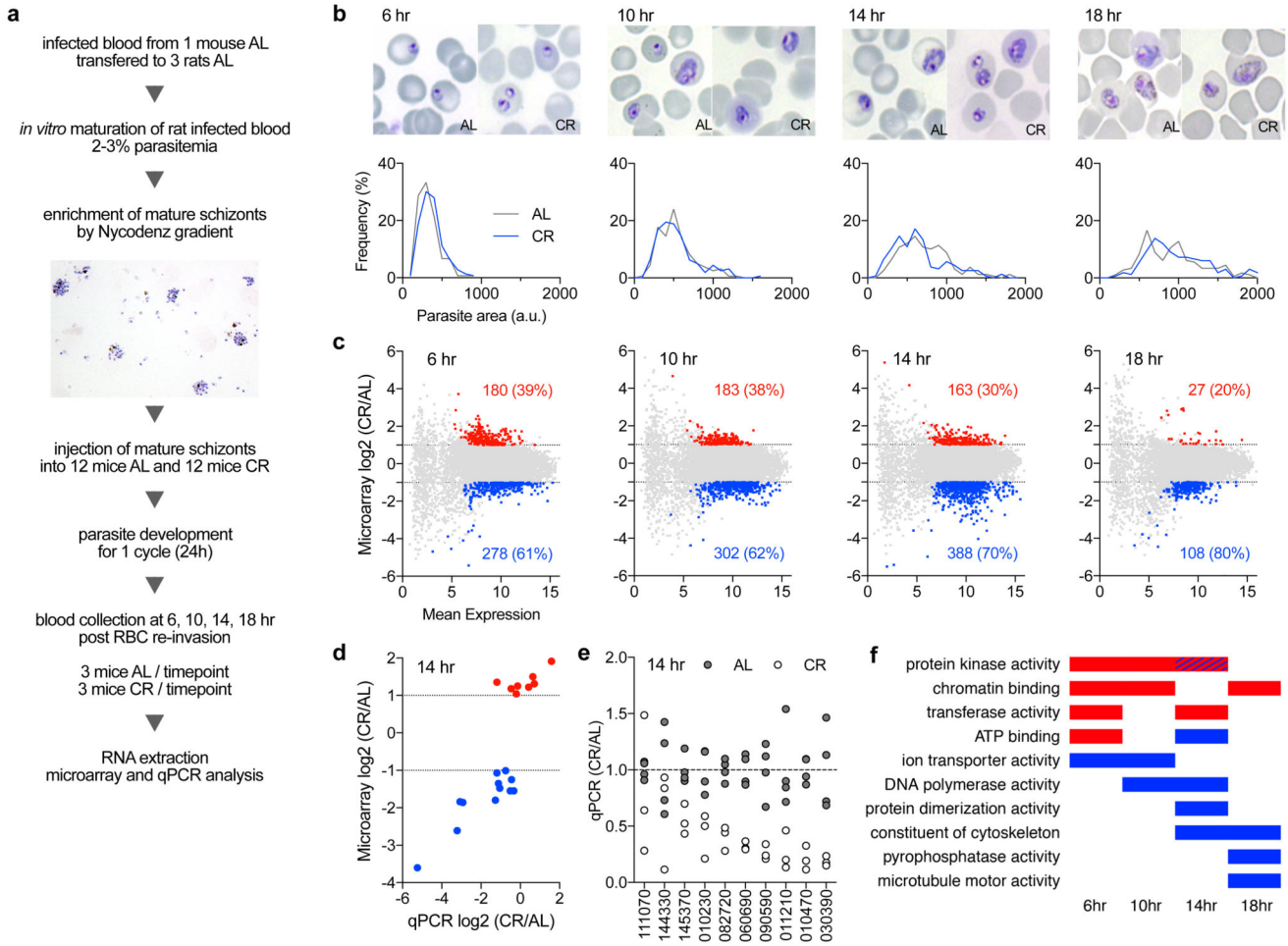

Extended Data Figure 3. Microarray analysis of *P. berghei* parasites under CR.

a. Schematic representation of parasite sample preparation for microarray time-course analysis. *P. berghei* ANKA parasites collected with 4 hr intervals 30 hr after intravenous injection of purified schizonts into AL and CR mice.

b. Microscopy analysis of parasite size (as proxy for parasite age) in the samples used in the microarrays show no apparent morphological differences in parasite development under AL and CR across the different time-points. The parasite area (a.u., arbitrary units) is defined by the Giemsa staining on thin blood smears following Lemieux et al., 200933 and was scored

Europe PMC Funders Author Manuscripts

using ImageJ. Histograms of parasite size distribution (3 mice/group/time-point). The total number of parasites analyzed are as follows: 6 hr, AL n=150, CR n=143; 10 hr, AL n=158, CR n=159; 14 hr, AL n=158, CR n=157; 18 hr, AL n=180, CR n=121). The indicated time-points correspond to the parasite developing time after RBC re-invasion, in the second cycle.

c. Scatter plots of log2 fold change (FC) (y-axis) and mean expression levels (x-axis) of parasites in CR *vs* AL (CR/AL) of 3 mice/group at the indicated time-points. Genes differentially induced or repressed in CR (with log2 FC of 1 and adjusted $p<0.01$) are highlighted in red and blue, respectively. The number (and relative percentage) of genes altered for each time-point is given in the graphs in red (induced) and blue (repressed).

d. Correlation plot between microarray and qPCR analysis for the 14-hour samples. 20 genes were selected based on the highest fold-changes, analyzed by qPCR and compared to the values obtained in the microarray analysis. Validation rate was 80%. Values are mean of 3 mice/group. The list of genes analyzed and their fold-changes in qPCR and microarray is given in the Source Data file.

e. qPCR analysis of repressed genes in independent biological samples collected at 14 hr (AL n=4, CR n=3). Each circle represents 1 mouse. Gene IDs are shown without their PBANKA_ prefix. Microarray hybridization was performed one time and confirmed by qPCR for a subset of genes in the same RNA samples (**d**), as well as independently collected samples (**e**).

f. Gene ontology enrichment analysis (Molecular Function) of the genes showing significant alterations for each time point using PlasmoDB (www.plasmodb.org) tools and considering Benjamini-Hochberg <0.05. The graph highlights the top 4 of terms with highest significance for each time point and/or terms that appear more than once. Red, induced; blue, repressed. The full list of terms (including Biological Process analysis) for each time point is given in the Source Data file.

Europe PMC Funders Author Manuscripts

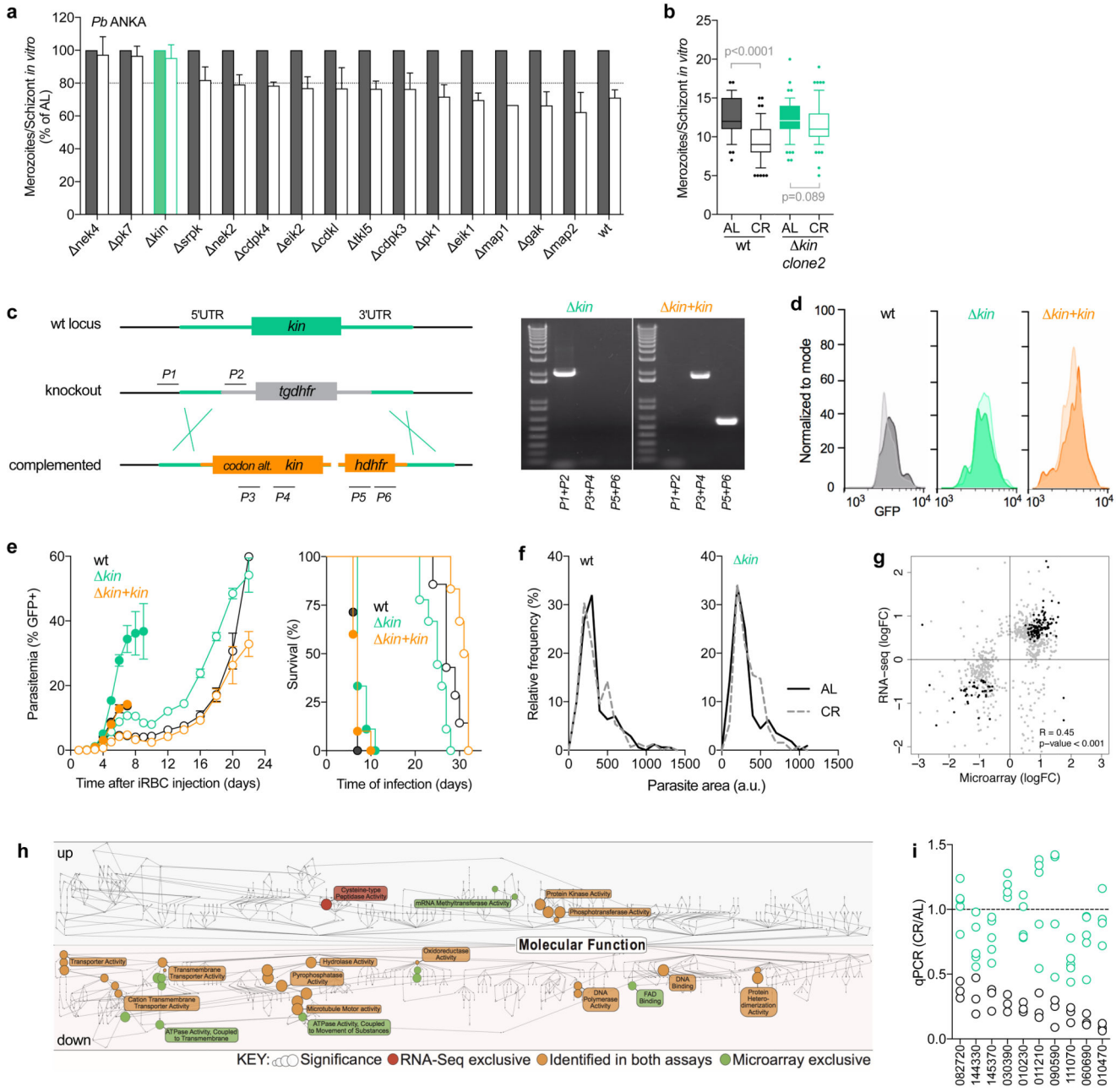

Extended Data Figure 4. Screen of *P. berghei* kinase mutants and characterization of Δ*kin* and complemented parasite lines.

a. Screening of kinase mutants using the CR *in vitro* assay. Screen performed in media supplemented with 25% of AL or CR sera (glucose, 4mM). The graph shows the relative reduction of merozoite formation in CR (unfilled bars) in comparison to AL (filled bars). Values are mean±sd of 3 independent experiments for wt, Δ*nek4,* Δ*pk7,* Δ*kin*, Δ*cdkl,* Δ*cdpk3,* Δ*gak,* Δ*tkl5* and 2 independent experiments for other knockout lines. The total number of schizonts analyzed is as follows: wt, AL n=150, CR n=167; Δ*kin,* AL n=80, CR n=86; Δ*pk1,* AL n=108, CR n=89; Δ*pk7,* AL n=134, CR n=154; Δ*nek2,* AL n=99, CR n=86;

Europe PMC Funders Author Manuscripts

Δ*nek4,* AL n=117, CR n=79; Δ*cdpk3,* AL n=46, CR n=81; Δ*cdpk4,* AL n=55, CR n=63; Δ*gak,* AL n=46, CR n=54; Δ*cdkl,* AL n=79, CR n=62; Δ*tkl5,* AL n=99, CR n=93; Δ*srpk,* AL n=59, CR n=86; Δ*eik1,* AL n=110, CR n=71; Δ*eik2,* AL n=116, CR n=84; Δ*map1,* AL n=90, CR n=59; Δ*map2,* AL n=50, CR n=42.

b. Boxplot of microscopic analysis of merozoite numbers for *P. berghei* ANKA wild-type (wt, AL n=49, CR n=77) and a second independent clone of Δ*kin* (AL n=54, CR n=73) in the same conditions as in (**a**) (Mann-Whitney test).

c. Schematic of Δ*kin* complementation strategy. Double crossover recombination at Pb*kin* 5' and 3' UTR was used to genetically delete the previously introduced tg*dhfr* and complement with codon-altered Pb*kin* gene and h*dhfr*. Transgenic parasites were selected by WR99210 treatment of mice (4 subcutaneous daily injections, 16mg/Kg/day). Annealing sites for genotyping primers are illustrated (left) and primer sequences are given in Supplementary Table 1. Agarose gel image (representative of 3) showing diagnostic PCR products from Δ*kin* and Δ*kin+kin* extracted genomic DNA, after dilution cloning of the complemented parasite line (right).

d. Flow cytometry analysis of GFP-expressing *P. berghei* ANKA wild-type, Δ*kin* and complemented Δ*kin* parasites after *in vitro* maturation to schizonts with medium supplemented with AL and CR sera as in (**a**) and analyzed as in Extended Data Fig. 2e. Histograms represent 2 independent experiments.

e. Full course parasitemia (mean±sem) and survival of C57BL/6 mice AL and CR infected by i.p. injection of 1×10^6 iRBCs of *P. berghei* wild-type (wt; AL n=7, CR n=7), Δ*kin* (AL n=9, CR n=8) and Δ*kin+kin* (AL n=10, CR n=6). AL, closed circles; CR, open circles.

f. Analysis of parasite area (arbitrary units, a.u.) on Giemsa-stained smears of the samples used for RNA sequencing, as in Extended Data Fig. 3b. Histograms of parasite size distribution (3 mice/group). The total number of parasites analyzed as follows: wt, AL n=172, CR n=148; Δ*kin*, AL n=112, CR n=129.

g. Correlation plot between microarray and RNA sequencing (RNAseq) analysis for the wild-type samples at 10 hr. Analysis of top 500 genes with $p<0.01$ in CR *vs* AL and expression levels higher than the first quartile in both platforms are shown in the graph. Despite the use of different platforms to analyze gene expression, there is 0.45 correlation between microarray and RNAseq data from the two independently obtained wild-type samples ($p < 0.001$).

h. Comparison of GO term enrichment analysis of CR-altered genes between RNAseq and microarray platforms for the 10 hr time-point. The GO "Molecular Function" graph highlights the location and relation of significantly enriched terms. As indicated in the key, node size refers to the level of significance of each GO term, while the color of the node represents if a particular term was detected in one or both platforms. The graph is split into two halves; where the top half represents the enrichment of terms from upregulated genes and the bottom half that of downregulated genes. Although the overlap between different transcriptomic methods was, as expected incomplete, this GO term enrichment analysis of the datasets revealed consistency in the functions of the genes that responded to CR.

i. qPCR analysis of *P. berghei* wt and Δ*kin* in independent biological samples. Data presented are mean±sem (wt, n=3/group; Δ*kin*, n=5/group), normalized to AL of the correspondent genotype. Each circle represents 1 mouse. Gene IDs are given without their PBANKA_ prefix. The genes analyzed were experimentally validated in Extended Data Fig.

3d-e and encode proteins related to lipid metabolism, members of transcriptional regulators (ApiAP2), and several transporters.

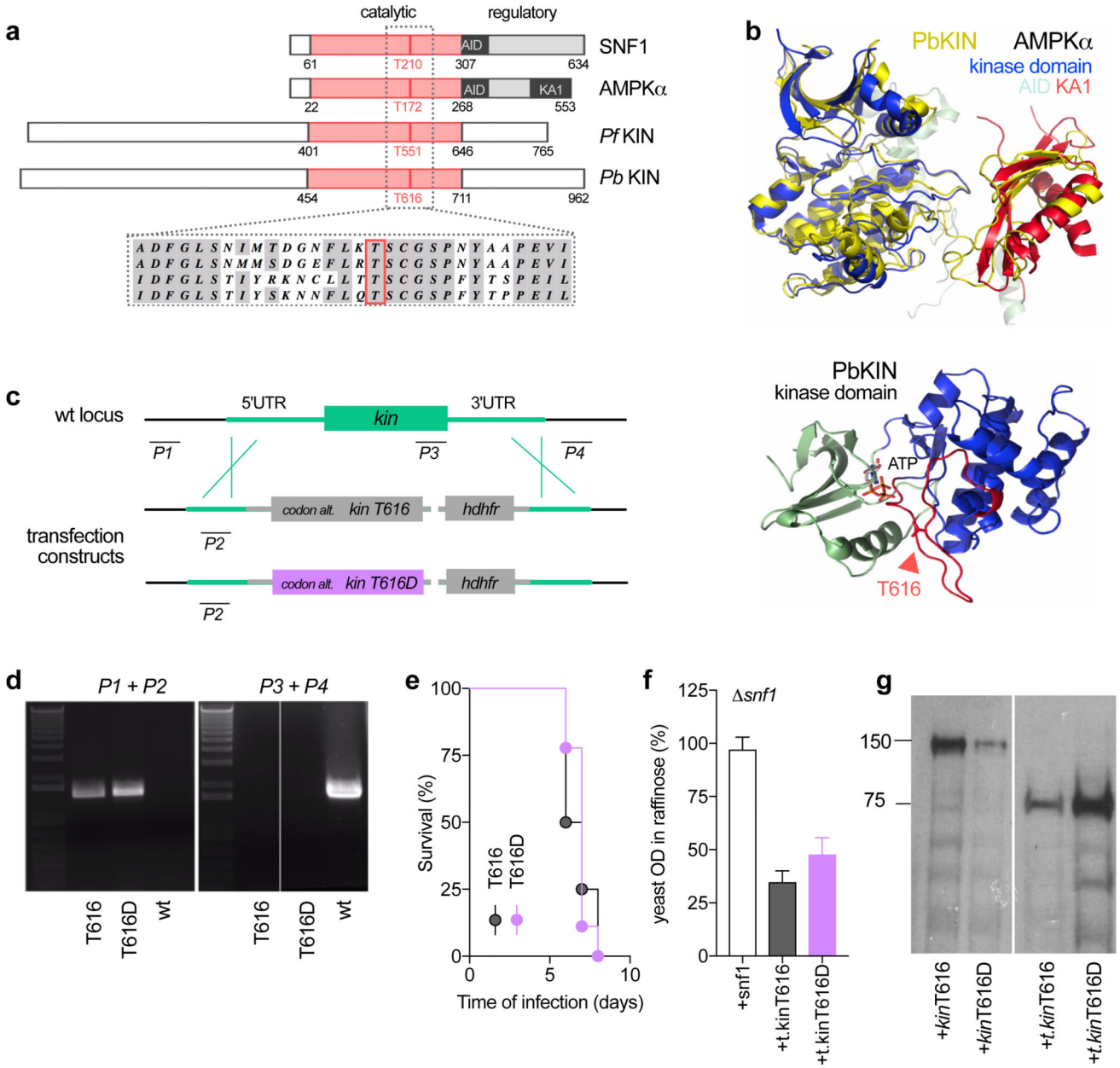

Extended Data Figure 5. PbKIN and PbKIN T616D phosphomimetic mutation.

a. Schematic diagram of yeast SNF1 and human AMPKα showing the conservation of *P. falciparum* and *P. berghei* KIN kinase catalytic domain (red). This kinase domain is flanked by an unusually long N-terminal region and a poorly conserved C-terminus, both with no obvious domains. Amino acid sequence alignment of the activation loop reveals a high degree of similarity and the conservation of the T-loop threonine (red line) whose

Europe PMC Funders Author Manuscripts

phosphorylation is essential for kinase activity. *AID,* autoinhibitory domain; *KA1,* Kinase Associated domain1.

b. Model of PbKIN on AMPKα (top) and PbKIN catalytic domain (bottom). The predicted amino acid sequence of PbKIN kinase domain (455-712) was used to generate a model by Phyre using the human AMPK structure (PDB: 4RER). The model is shown in cartoon representation and depicts the small lobe (455-539) in green, the large lobe (540-712) in blue and the T-loop (601-626) in red with the T616 in sticks. An ATP molecule (stick representation) was docked to illustrate the catalytic site with Lysine 489 (stick representation). Both the AID and the KA1 domain were also modeled but it appeared not to be conserved.

c. Schematic for the generation of *P. berghei* KIN^{T616} and KIN^{T616D} mutant. Double cross-over recombination at 5' and 3' UTR was used to genetically delete endogenous *kin* and complement with codon-altered *kin* gene encoding wild-type (KIN^{T616}) or phosphomimetic mutation (KIN^{T616D}). Codon-altered sequence of *Pbkin* was obtained from GenScript, which was then used in the site-directed mutagenesis reaction to introduce the T616D mutation. Presence of codon-altered *kin^{T616}* and *kin^{T616D}* was confirmed by sequencing of the locus of the transgenic parasites. Annealing sites for genotyping primers are illustrated and primer sequences are given in Supplementary Table 1.

d. Agarose gel image (representative of 2) showing diagnostic PCR products from *P. berghei* KIN^{T616}, KIN^{T616D} and parental wild-type.

e. Survival of C57BL/6 mice infected by i.p. injection (1×10^6 iRBC/mouse) of *P. berghei* KIN^{T616} (n=9) and KIN^{T616D} (n=9).

f. Complementation of the Δ*snf1* yeast mutant with GFP-fused yeast-optimized sequences of N-terminal truncated *P. berghei kin*^{T616}, *kin*^{T616D} or yeast *snf1* without GFP tag. Truncation is indicated with a *t.* Growth of transformed Δ*snf1* cells in culture, inoculated at a density of 0.05 OD_{600} in SD medium supplemented with glucose or raffinose as a carbon source and grown for 42h. Shown are OD values obtained in the raffinose condition, normalized to those obtained in glucose condition for each cell line (*snf1* n=6, *t.kin*^{T616} n=6, *t.kin*^{T616D} n=6; mean±sem; Mann-Whitney test).

g. Western blot analysis of Δ*snf1* expressing full length (left) or N-terminal truncated (right) *Pb*KIN^{T616}-GFP or *Pb*KIN^{T616D}-GFP. Predicted size of full length *Pb*KIN-GFP is 147 kDa and of N-terminal truncated version is 93 kDa. Membranes were probed with anti-GFP antibody. Truncations are indicated with a *t.* A representative blot from 2 independent lysates is shown.

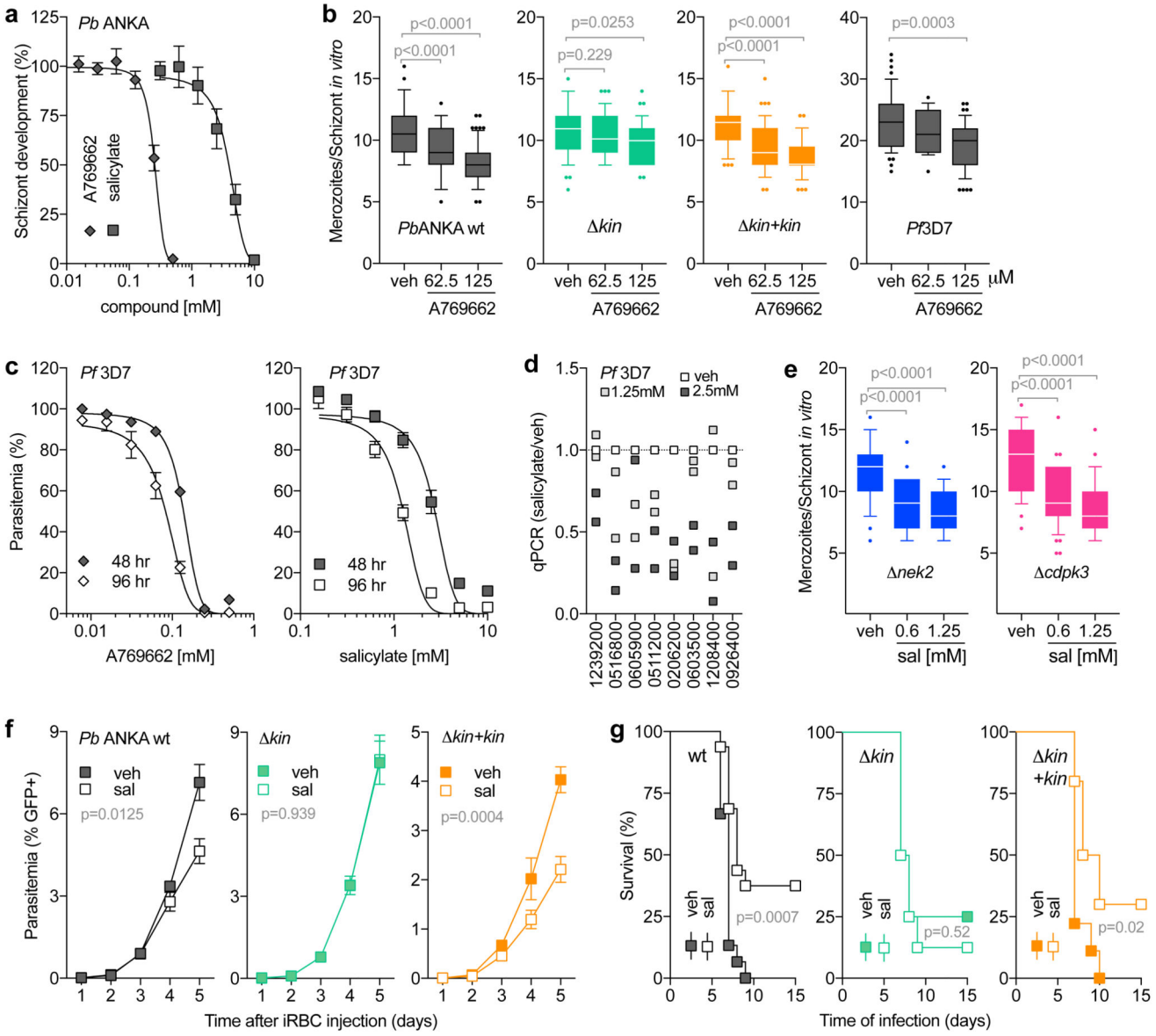

Extended Data Figure 6. Effect of AMPK agonists.

a. Dose-dependent effect of AMPK activators (salicylate and A769662) on *P. berghei* ANKA that express luciferase (under *ama1* schizont-specific promoter). Parasites were cultured for 24 hr with increasing concentrations of the compounds (media supplemented with 20% FBS and 5mM glucose). Analysis of schizont development was performed by measuring luminescence. Values are mean±sem (salicylate, n=5; A769662, n=6). EC50 values determined by using GraphPad Prism non-linear regression variable slope (normalized) analysis. The calculated EC50 values are as follows: salicylate, 2.4±0.9 mM; A769662, 256.5±60.6 µM.

b. Dose-dependent effect of A769662 on *P. falciparum*, *P. berghei* ANKA wild-type, Δ*kin* and complemented parasites analyzed by microscopy after Giemsa staining (Mann-Whitney test). Boxplots show the data for the following number of schizonts (vehicle, A769662 62.5

Europe PMC Funders Author Manuscripts

Europe PMC Funders Author Manuscripts

and 125 μM): *P. falciparum,* 59, 18, 48; *P. berghei* wt, 28, 68, 61; Δ*kin,* 44, 47, 40; Δ*kin+kin,* 34, 57, 37.

c. Dose-dependent effect of A769662 and salicylate treatments on *P. falciparum* for 2 developmental cycles. Synchronized cultures were set at 0.1% initial parasitemia (rings) and analyzed at 48 hr and 96 hr by flow cytometry after SYBR Green labeling of parasite DNA. A new generation of rings was observed at 48 and 96 hr in the treated conditions, suggesting no growth delay. Data (mean±sem) was normalized to the untreated control on each experiment at 48hr or 96hr. The EC50 values (determined as in **a**) are as follows: 133.1±3.4μM at 48 hr (n=6) and 70.1±18.9μM at 96 hr (n=5) for A769662; 2.2±0.2mM at 48 hr (n=6) and 1.25±0.2mM at 96 hr (n=6) for salicylate.

d. qPCR analysis of *P. falciparum* parasites treated with salicylate for 72 hr (n=2/condition). Data normalized to the untreated control. The genes analyzed correspond to the *P. berghei* homologues experimentally validated in Extended Data Fig. 3. Gene IDs are shown in the figure without their PF3D7_ prefix.

e. Dose-dependent effect of salicylate on other *P. berghei* ANKA kinase mutants. Boxplot of parasites treated and analyzed as in (**a**) (Mann-Whitney test). The number of schizonts analyzed for vehicle, 0.6 mM and 1.25mM are as follows: Δ*nek2,* 43, 33, 37; Δ*cdpk3,* 35, 44, 30.

f-g. Salicylate effect *in vivo*. Mice were treated daily with 250mg/kg salicylate (sal) or 0.9% NaCl (vehicle, veh) starting at day 1 after infection. Parasitemia (mean±sem; 2-way ANOVA test) and survival (log-rank Matel-Cox test) of C57BL/6 mice infected by i.p. injection of 1×10^6 wt (veh n=15; sal n=16), Δ*kin* (veh n=8; sal n=8) and complemented Δ*kin+kin* iRBCs (veh n=10; sal n=10).

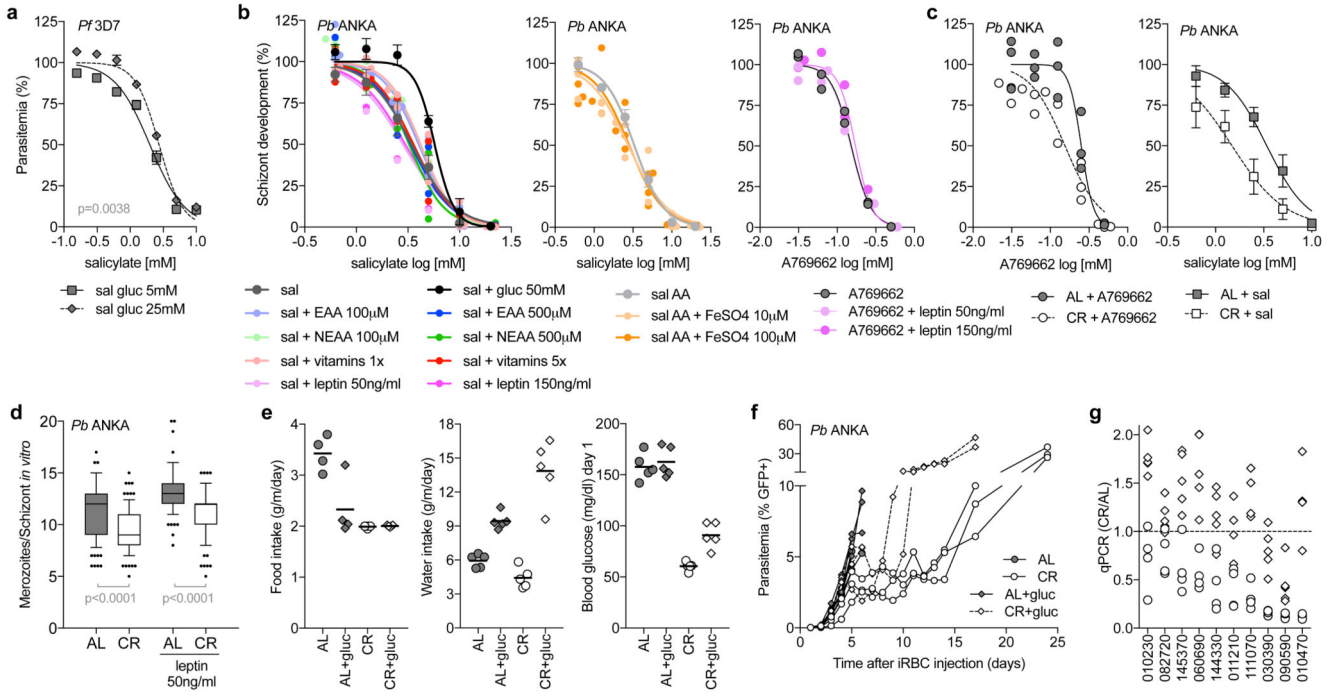

Extended Data Figure 7. Supplementation studies *in vitro* and *in vivo*.

a. Effect of glucose supplementation on salicylate-treated *P. falciparum* parasites. Ring-stage synchronized cultures were set at 0.1% initial parasitemia in a glucose free medium supplemented with 5 and 25mM glucose. Values in the graph are parasitemia (mean±sem; n=5/condition) determined by flow cytometry after staining with SYBR Green at 48 hr. Salicylate EC50 values were 2.0±0.1 mM and 2.7±0.2 mM for 5 and 25mM glucose, respectively. P value in the figure calculated with 2-way ANOVA test.

b. Effect of supplementation with extra glucose, vitamins, essential amino acids (EAA), non-essential (NEAA), leptin and iron ($FeSO_4$) on salicylate- or A769662-treated parasites. *P. berghei* expressing luciferase at schizont stage were cultured in 20% FBS supplemented medium (5mM glucose, n=5) with increasing concentrations of salicylate and extra glucose (50mM, n=5), vitamins (1x, n=3; 5x, n=2), EAA (100μM, n=3; 500μM, n=2), NEAA (100μM, n=3; 500μM, n=2), and leptin (50ng/ml, n=2; 150ng/ml n=2). $FeSO_4$ was added in the presence of equal amount of ascorbic acid (AA), an iron absorption enhancer. A769662 treatments were conducted in 20% FBS supplemented medium (5mM glucose) and leptin (50ng/ml, n=2; 150ng/ml n=2). Analysis of schizont development was performed by measuring luciferase activity as in Fig. 1f. Values normalized to the vehicle control. Replicates are shown as individual data points for all supplementations except 50mM glucose, AA and salicylate alone, which are shown as mean±sem. Salicylate EC50 values in these experiments were 3.4±0.3 mM and 5.7±1.3 mM for 5 and 50mM glucose, respectively (p=0.0081, 2-way ANOVA test).

c. Dose-dependent effect of salicylate and A769662 on *P. berghei* parasites in the presence of AL or CR sera. Parasites were incubated for 24 hr with increasing concentrations of the compounds in media supplemented with 10% of AL or CR sera (glucose 5mM). Analysis of schizont development was performed by measuring luminescence (A769662, n=3; salicylate, n=5). These compounds appear to have additive effects, suggesting that under CR conditions, A769662/salicylate might activate KIN through distinct and/or complementary mechanisms. This could be related to different binding sites on the kinase, as previously demonstrated for other AMPKs23,24.

d. Boxplot of microscopic analysis of *P. berghei* ANKA wild-type segmented schizonts obtained *in vitro* after 24hr maturation in the presence of AL or CR sera. Recombinant leptin was added to the culture medium at the indicated concentration. Total number of schizonts analyzed in 2 independent experiments as follows: AL, 87; CR, 85; AL+Leptin, 69; CR, 86 (Mann-Whitney test).

e-g. Effect of glucose supplementation on C57BL/6 male mice in CR or AL. 0.2g/mL of glucose was provided in the drinking water starting on the day of infection.

e. Average daily food consumption and water intake for the same group of mice. Blood glucose levels after 20 hr of glucose supplementation. Representative of 2 independent experiments (AL n=5, CR n=4, AL+glucose n=5, CR+glucose n=5).

f. Parasitemia of C57BL/6 mice AL or CR and glucose supplemented groups, infected by i.p. injection of 1×10^6 iRBCs of GFP-expressing *P. berghei* wild-type parasites. Data represent 1 of 2 independent experiments (n=3/group). Each mouse is plotted as an individual data point.

g. qPCR analysis of *P. berghei* wild-type parasites in AL or CR fed C57BL/6 mice supplemented (diamonds; n=5) or not (circles; n=4) with glucose in drinking water. Shown is parasite relative gene expression in CR normalized to the mean of the correspondent AL

condition at day 5 after i.p. infection. Each mouse is plotted as an individual data point. Representative of 2 experiments performed independently. Gene IDs are given without their PBANKA_ prefix as in Extended Data Fig. 3e.

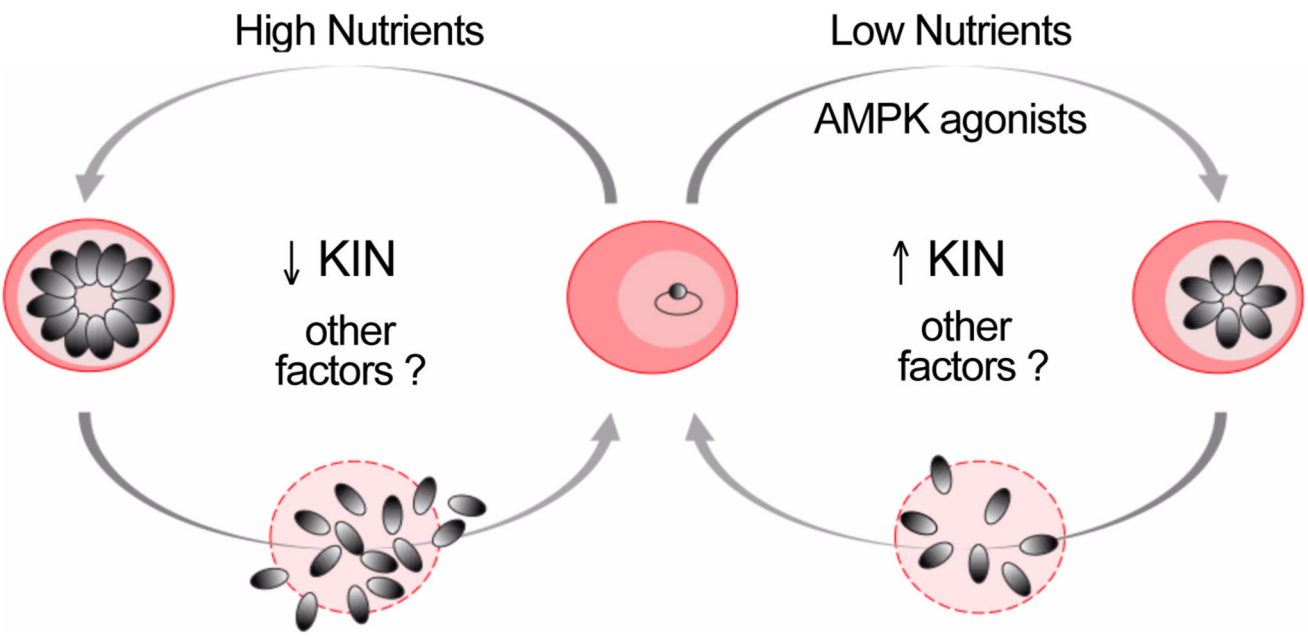

Extended Data Figure 8.

Schematic representation of the observed effect of dietary nutrients or AMPK agonists on *Plasmodium* intraerythrocytic replication. The data supports the idea that parasites can replicate in higher or fewer numbers depending on host nutrient availability. This active parasite response mediated by an AMPKα-related kinase, KIN, which is expected to become active by an increase of the AMP:ATP ratio in parasites facing nutrient deficiency. KIN upstream regulators and downstream targets remain to be determined, as well as other potential molecular factors that might also contribute to this nutrient sensing mechanism.

Supplementary Material

Refer to Web version on PubMed Central for supplementary material.

Acknowledgments

We thank Ana Pena and Ana Pamplona for help with animal experiments; Sofia Marques for help in transfections; Ana Parreira for the mosquito preparation; Maria Rebelo for help with flow cytometry analysis; Thomas Hanscheid and Francisco Enguita for helpful discussions; Richard Wall and Declan Brady for technical assistance with Δ*kin* clones; and Jacobus Pharmaceuticals for the WR99210 compound. The work was supported by European Research Council (311502) and Fundação para a Ciência e Tecnologia (FCT) grants (EXCL/IMI-MIC/0056/2012) and (PTDC/SAU-MET/118199/2010) to M.M.M. and L.M.S., respectively. L.M.S., A.R.G.2 and M.M.M. were supported by the European Commission (FP7/2007-2013; EVIMALAR 242095). L.M.S. was supported by EMBO LTF (ALTF 960-2009). K.S. was sponsored by FCT fellowship (SFRH/BPD/111788/2015). I.M.V. received EMBO (LTF 712-2012) and NIH NRSA (5F32AI104252-03) fellowships. Work at the Sanger Institute was funded by Wellcome Trust (098051) and Medical Research Council (MRC, G0501670). Work at the Instituto Gulbenkian de Ciência was funded through FCT grants (SFRH-BPD79255-2011 and UID/Multi/04551/2013). R.T. was supported by MRC grant (G0900109, MR/K011782/1). M.L. was funded through the Burroughs Welcome Fund and the NIH Director's New Innovators award (1DP2OD001315-01).

References

1. Efeyan A, Comb WC, Sabatini DM. Nutrient-sensing mechanisms and pathways. Nature. 2015; 517:302–310. DOI: 10.1038/nature14190 [PubMed: 25592535]
2. Chantranupong L, Wolfson RL, Sabatini DM. Nutrient-sensing mechanisms across evolution. Cell. 2015; 161:67–83. DOI: 10.1016/j.cell.2015.02.041 [PubMed: 25815986]
3. Babbitt SE, et al. Plasmodium falciparum responds to amino acid starvation by entering into a hibernatory state. Proc Natl Acad Sci U S A. 2012; 109:E3278–3287. DOI: 10.1073/pnas.1209823109 [PubMed: 23112171]
4. Miranda-Saavedra D, Gabaldon T, Barton GJ, Langsley G, Doerig C. The kinomes of apicomplexan parasites. Microbes Infect. 2012; 14:796–810. DOI: 10.1016/j.micinf.2012.04.007 [PubMed: 22587893]
5. Serfontein J, Nisbet RE, Howe CJ, de Vries PJ. Evolution of the TSC1/TSC2-TOR signaling pathway. Sci Signal. 2010; 3:ra49.doi: 10.1126/scisignal.2000803 [PubMed: 20587805]
6. Collino S, et al. Transcriptomics and Metabonomics Identify Essential Metabolic Signatures in Calorie Restriction (CR) Regulation across Multiple Mouse Strains. Metabolites. 2013; 3:881–911. DOI: 10.3390/metabo3040881 [PubMed: 24958256]
7. Fontana L, Meyer TE, Klein S, Holloszy JO. Long-term calorie restriction is highly effective in reducing the risk for atherosclerosis in humans. Proc Natl Acad Sci U S A. 2004; 101:6659–6663. DOI: 10.1073/pnas.0308291101 [PubMed: 15096581]
8. Fontana L, Partridge L, Longo VD. Extending healthy life span--from yeast to humans. Science. 2010; 328:321–326. DOI: 10.1126/science.1172539 [PubMed: 20395504]
9. Meidenbauer JJ, Ta N, Seyfried TN. Influence of a ketogenic diet, fish-oil, and calorie restriction on plasma metabolites and lipids in C57BL/6J mice. Nutr Metab (Lond). 2014; 11:23.doi: 10.1186/1743-7075-11-23 [PubMed: 24910707]
10. Hunt NH, Manduci N, Thumwood CM. Amelioration of murine cerebral malaria by dietary restriction. Parasitology. 1993; 107(Pt 5):471–476. [PubMed: 8295786]
11. Mejia P, et al. Dietary restriction protects against experimental cerebral malaria via leptin modulation and T-cell mTORC1 suppression. Nat Commun. 2015; 6:6050.doi: 10.1038/ncomms7050 [PubMed: 25636003]
12. Pasini EM, et al. Proteomic and genetic analyses demonstrate that Plasmodium berghei blood stages export a large and diverse repertoire of proteins. Mol Cell Proteomics. 2013; 12:426–448. DOI: 10.1074/mcp.M112.021238 [PubMed: 23197789]
13. Gasch, AP. Yeast Stress Responses. Hohmann, Stefan, Mager, Willem H., editors. Springer; 2003. Ch. 2
14. Tewari R, et al. The systematic functional analysis of Plasmodium protein kinases identifies essential regulators of mosquito transmission. Cell Host Microbe. 2010; 8:377–387. DOI: 10.1016/j.chom.2010.09.006 [PubMed: 20951971]
15. Dorin-Semblat D, Sicard A, Doerig C, Ranford-Cartwright L, Doerig C. Disruption of the PfPK7 gene impairs schizogony and sporogony in the human malaria parasite Plasmodium falciparum. Eukaryot Cell. 2008; 7:279–285. DOI: 10.1128/EC.00245-07 [PubMed: 18083830]
16. Mony BM, et al. Genome-wide dissection of the quorum sensing signalling pathway in Trypanosoma brucei. Nature. 2014; 505:681–685. DOI: 10.1038/nature12864 [PubMed: 24336212]
17. Bracchi V, Langsley G, Thelu J, Eling W, Ambroise-Thomas P. PfKIN, an SNF1 type protein kinase of Plasmodium falciparum predominantly expressed in gametocytes. Mol Biochem Parasitol. 1996; 76:299–303. [PubMed: 8920016]
18. Hardie DG, Ross FA, Hawley SA. AMP-activated protein kinase: a target for drugs both ancient and modern. Chem Biol. 2012; 19:1222–1236. DOI: 10.1016/j.chembiol.2012.08.019 [PubMed: 23102217]
19. Crozet P, et al. Mechanisms of regulation of SNF1/AMPK/SnRK1 protein kinases. Front Plant Sci. 2014; 5:190.doi: 10.3389/fpls.2014.00190 [PubMed: 24904600]
20. Boehme, U., Otto, TD., Cotton, J., Steinbiss, S., Sanders, M., Oyola, SO., Nicot, A., Gandon, S., Patra, KP., Herd, C., Bushell, E., et al. Complete avian malaria parasite genomes reveal host-

specific parasite evolution in birds and mammals. 2016. http://biorxiv.org/content/early/2016/11/09/086504

21. Stein SC, Woods A, Jones NA, Davison MD, Carling D. The regulation of AMP-activated protein kinase by phosphorylation. The Biochemical journal. 2000; 345(Pt 3):437–443. [PubMed: 10642499]
22. Hawley SA, et al. The ancient drug salicylate directly activates AMP-activated protein kinase. Science. 2012; 336:918–922. DOI: 10.1126/science.1215327 [PubMed: 22517326]
23. Calabrese MF, et al. Structural basis for AMPK activation: natural and synthetic ligands regulate kinase activity from opposite poles by different molecular mechanisms. Structure. 2014; 22:1161–1172. DOI: 10.1016/j.str.2014.06.009 [PubMed: 25066137]
24. Xiao B, et al. Structural basis of AMPK regulation by small molecule activators. Nat Commun. 2013; 4:3017.doi: 10.1038/ncomms4017 [PubMed: 24352254]
25. Pankevich DE, Teegarden SL, Hedin AD, Jensen CL, Bale TL. Caloric restriction experience reprograms stress and orexigenic pathways and promotes binge eating. J Neurosci. 2010; 30:16399–16407. DOI: 10.1523/JNEUROSCI.1955-10.2010 [PubMed: 21123586]
26. Murray MJ, Murray NJ, Murray AB, Murray MB. Refeeding-malaria and hyperferraemia. Lancet. 1975; 1:653–654. [PubMed: 47080]
27. Collaboration, N. C. D. R. F. Trends in adult body-mass index in 200 countries from 1975 to 2014: a pooled analysis of 1698 population-based measurement studies with 19.2 million participants. Lancet. 2016; 387:1377–1396. DOI: 10.1016/S0140-6736(16)30054-X [PubMed: 27115820]
28. Bousema T, Okell L, Felger I, Drakeley C. Asymptomatic malaria infections: detectability, transmissibility and public health relevance. Nat Rev Microbiol. 2014; 12:833–840. DOI: 10.1038/nrmicro3364 [PubMed: 25329408]
29. Janse CJ, Ramesar J, Waters AP. High-efficiency transfection and drug selection of genetically transformed blood stages of the rodent malaria parasite Plasmodium berghei. Nat Protoc. 2006; 1:346–356. DOI: 10.1038/nprot.2006.53 [PubMed: 17406255]
30. Franke-Fayard B, et al. Murine malaria parasite sequestration: CD36 is the major receptor, but cerebral pathology is unlinked to sequestration. Proc Natl Acad Sci U S A. 2005; 102:11468–11473. DOI: 10.1073/pnas.0503386102 [PubMed: 16051702]
31. Liu Y, Xu X, Carlson M. Interaction of SNF1 protein kinase with its activating kinase Sak1. Eukaryot Cell. 2011; 10:313–319. DOI: 10.1128/EC.00291-10 [PubMed: 21216941]
32. Gietz RD, Schiestl RH. Quick and easy yeast transformation using the LiAc/SS carrier DNA/PEG method. Nat Protoc. 2007; 2:35–37. DOI: 10.1038/nprot.2007.14 [PubMed: 17401335]
33. Lemieux JE, et al. Statistical estimation of cell-cycle progression and lineage commitment in Plasmodium falciparum reveals a homogeneous pattern of transcription in ex vivo culture. Proc Natl Acad Sci U S A. 2009; 106:7559–7564. DOI: 10.1073/pnas.0811829106 [PubMed: 19376968]
34. Kafsack BF, Painter HJ, Llinas M. New Agilent platform DNA microarrays for transcriptome analysis of Plasmodium falciparum and Plasmodium berghei for the malaria research community. Malar J. 2012; 11:187.doi: 10.1186/1475-2875-11-187 [PubMed: 22681930]
35. Kim D, et al. TopHat2: accurate alignment of transcriptomes in the presence of insertions, deletions and gene fusions. Genome Biol. 2013; 14:R36.doi: 10.1186/gb-2013-14-4-r36 [PubMed: 23618408]
36. Robinson MD, McCarthy DJ, Smyth GK. edgeR: a Bioconductor package for differential expression analysis of digital gene expression data. Bioinformatics. 2010; 26:139–140. DOI: 10.1093/bioinformatics/btp616 [PubMed: 19910308]
37. Ritchie ME, et al. limma powers differential expression analyses for RNA-sequencing and microarray studies. Nucleic Acids Res. 2015; 43:e47.doi: 10.1093/nar/gkv007 [PubMed: 25605792]
38. McCarthy DJ, Chen Y, Smyth GK. Differential expression analysis of multifactor RNA-Seq experiments with respect to biological variation. Nucleic Acids Res. 2012; 40:4288–4297. DOI: 10.1093/nar/gks042 [PubMed: 22287627]

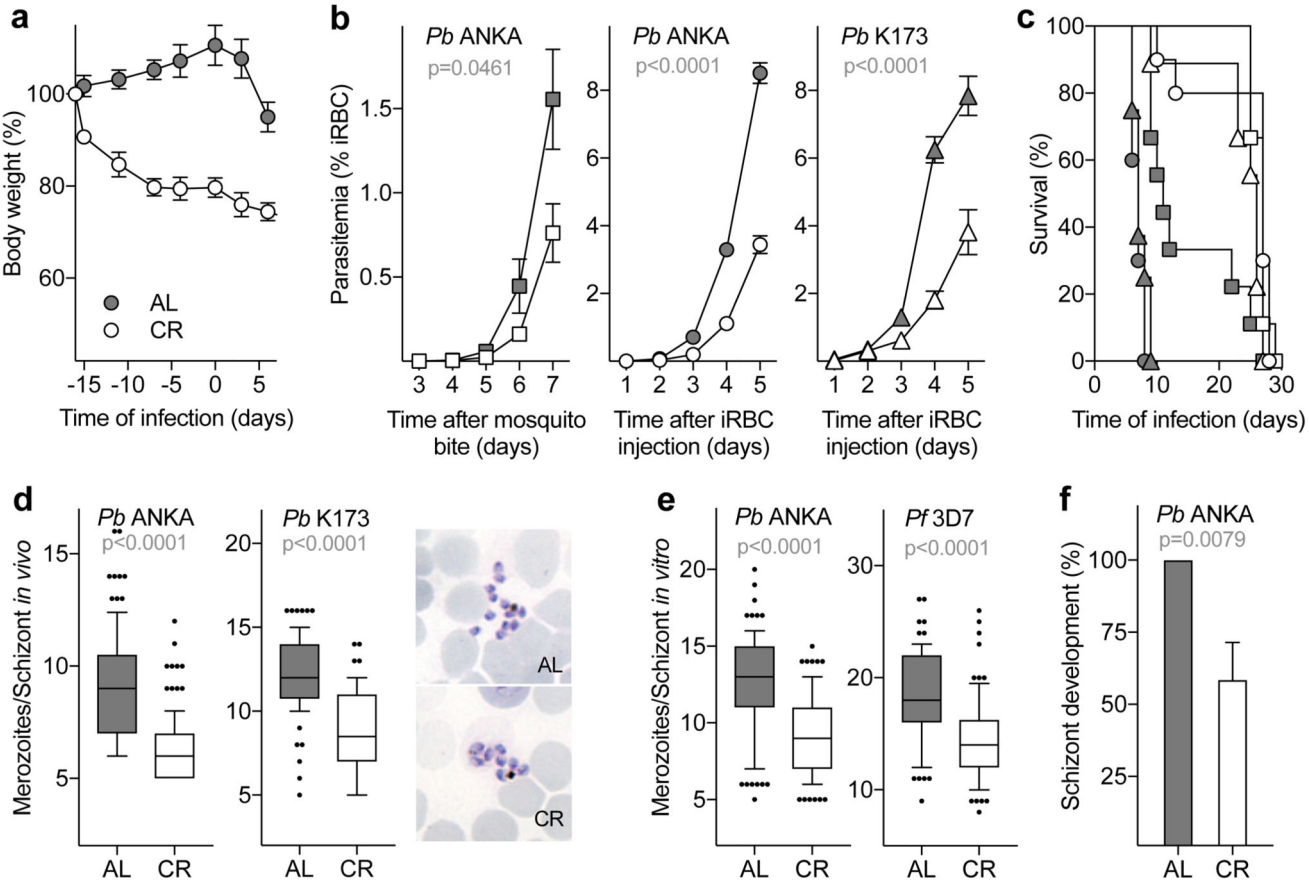

Figure 1. Host diet impacts survival and parasite replication.

a. Body weight change (mean±sd; n=8 mice/group) of C57BL/6 mice under long-term CR, normalized to initial weight. **b.** Parasitemia (mean±sem; 2-way ANOVA) and **c.** survival of C57BL/6 mice infected by mosquito bite (squares, AL n=9, CR n=9) or injection of iRBC obtained from AL mice (ANKA, circles, AL n=10, CR n=10; K173, triangles, AL n=8, CR n=9). **d.** Boxplot of merozoites numbers/schizont (Mann-Whitney) of *P. berghei* ANKA (AL n=105, CR n=137) and K173 (AL n=70, CR n=50, representative images shown) in mice (**d**) and *P. berghei* ANKA (AL n=110, CR n=106) and *P. falciparum* (AL n=71, CR n=74) after *in vitro* culture with AL or CR sera (**e**). **f.** Luminescence analysis of schizont-specific luciferase-expressing parasites after *in vitro* maturation (mean±sem; n=5; Mann-Whitney).

Europe PMC Funders Author Manuscripts

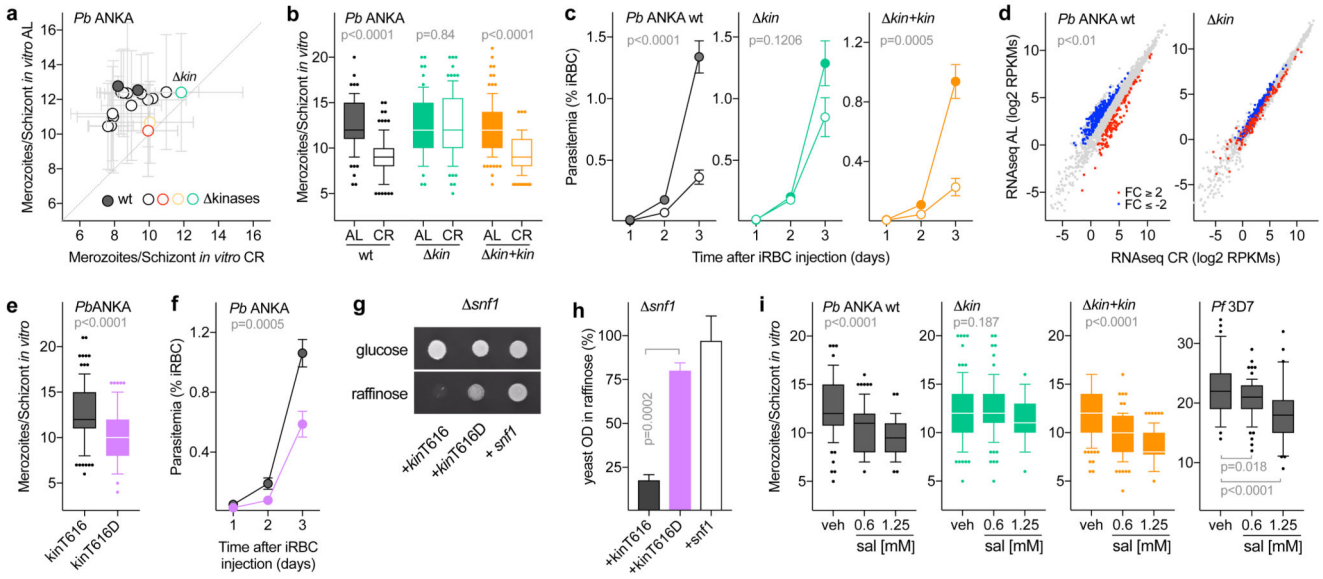

Figure 2. PbKIN mediates parasite response to CR.

a. Merozoite numbers (mean±sd) in AL and CR of 15 kinase knockout lines. Parasites in green (Δ*kin*; PBANKA_131800), red (Δ*pk7;* PBANKA_031030) and yellow (Δ*nek4;* PBANKA_061670) do not reduce replication in CR. **b.** Boxplot of wild-type (AL n=79, CR n=105), Δ*kin* (AL n=62, CR n=85) and Δ*kin+kin* (AL n=108, CR n=124) cultured as in (**a**) (Mann-Whitney). **c.** Parasitemia (mean±sem; 2-way ANOVA) of C57BL/6 mice infected with wild-type (AL n=10, CR n=11), Δ*kin* (AL n=13, CR n=12) and Δ*kin+kin* (AL n=10, CR n=6). **d.** RNA-sequencing analysis of wild-type and Δ*kin* (n=3 mice/group). **e.** Boxplot of KIN^{T616} (n=204) and KIN^{T616D} (n=136) cultured in FBS supplemented medium (Mann-Whitney). **f.** Parasitemia (mean±sem; 2-way ANOVA) of AL C57BL/6 mice infected with KIN^{T616} (n=9) and KIN^{T616D} (n=9). **g-h.** Complementation of Δ*snf1* yeast with *kin*^{T616}, *kin*^{T616D} and *snf1* shown on agar spots (1 of 2 representative images) and liquid growth in raffinose normalized to glucose (n=6/condition; mean±sem; Mann-Whitney). **i.** Boxplot of salicylate treatments. Number of schizonts analyzed for vehicle (veh), 0.6 and 1.25mM as follows: *P. berghei* wt, 74, 87, 56; Δ*kin,* 87, 92, 82; Δ*kin+kin,* 93, 75, 86; *P. falciparum*, 75, 69, 61 (Mann-Whitney).

Europe PMC Funders Author Manuscripts

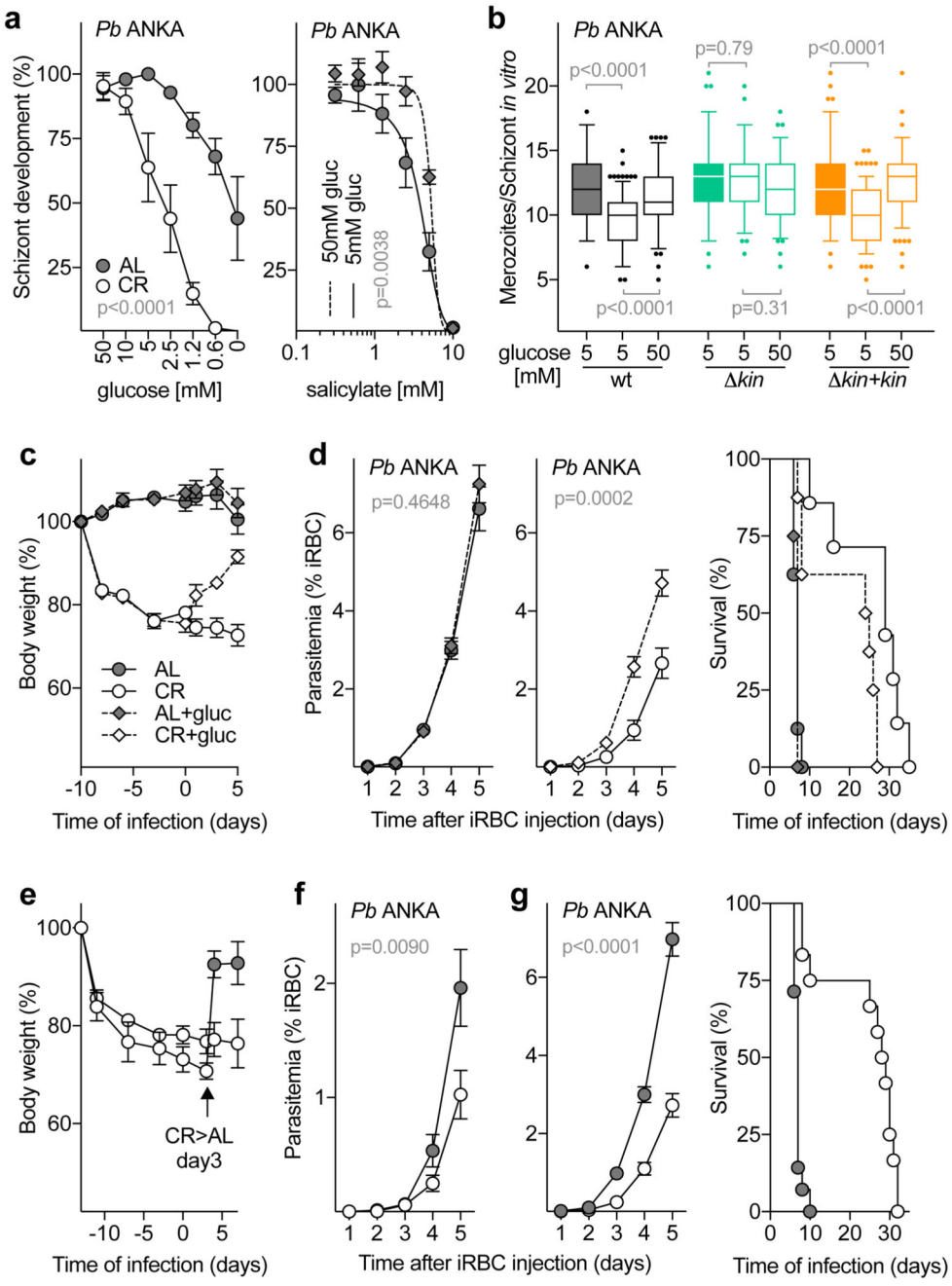

Figure 3. Glucose supplementation and re-feeding abolish CR effects.

a. Schizont maturation in glucose-free media supplemented with glucose and AL/CR sera (n=6), or FBS and salicylate (n=5). Data normalized to 5mM glucose (mean±sem; 2-way ANOVA). **b.** Boxplot of parasites cultured as in (**a**). Number of schizonts analyzed for AL 5mM, CR 5mM and CR 50mM as follows: wt, 50, 93, 87; Δ*kin,* 84, 71, 41; Δ*kin+kin,* 105, 86, 71 (Mann-Whitney). **c-d.** Body weight change (mean±sd), parasitemia (mean±sem; 2-way ANOVA) and survival of C57BL/6 mice with and without glucose supplementation (0.2g/mL drinking water) starting on the day of infection (AL n=8, CR n=7, AL+glucose

n=8, CR+glucose n=8). **e-f.** Body weight change (mean±sd; n=9/group) and parasitemia (mean±sem; n=13/group; 2-way ANOVA) of BALB/c mice in CR and after change to AL on day 3 after infection. **g.** Parasitemia (mean±sem; 2-way ANOVA) and survival of C57BL/6 mice infected with parasites derived from a CR mouse (AL n=14, CR n=12).

Europe PMC Funders Author Manuscripts